frontiers in MICROBIOLOGY

ORIGINAL RESEARCH ARTICLE
published: 14 May 2013
doi: 10.3389/fmicb.2013.00117

Increased infectivity in human cells and resistance to antibody-mediated neutralization by truncation of the SIV gp41 cytoplasmic tail

Takeo Kuwata[1], Kaori Takaki[1], Ikumi Enomoto[1], Kazuhisa Yoshimura[2] and Shuzo Matsushita[1]*

[1] Center for AIDS Research, Kumamoto University, Kumamoto, Japan
[2] AIDS Research Center, National Institute of Infectious Diseases, Tokyo, Japan

Edited by:
Akio Adachi, The University of Tokushima Graduate School, Japan

Reviewed by:
Tetsuro Matano, University of Tokyo, Japan
Tsutomu Murakami, National Institute of Infectious Diseases, Japan
Hirofumi Akari, Kyoto University, Japan

***Correspondence:**
Shuzo Matsushita, Center for AIDS Research, Kumamoto University, 2-2-1 Honjo, Chuo-ku, Kumamoto 860-0811, Japan.
e-mail: shuzo@kumamoto-u.ac.jp

The role of antibodies in protecting the host from human immunodeficiency virus type 1 (HIV-1) infection is of considerable interest, particularly because the RV144 trial results suggest that antibodies contribute to protection. Although infection of non-human primates with simian immunodeficiency virus (SIV) is commonly used as an animal model of HIV-1 infection, the viral epitopes that elicit potent and broad neutralizing antibodies to SIV have not been identified. We isolated a monoclonal antibody (MAb) B404 that potently and broadly neutralizes various SIV strains. B404 targets a conformational epitope comprising the V3 and V4 loops of Env that intensely exposed when Env binds CD4. B404-resistant variants were obtained by passaging viruses in the presence of increasing concentration of B404 in PM1/CCR5 cells. Genetic analysis revealed that the Q733stop mutation, which truncates the cytoplasmic tail of gp41, was the first major substitution in Env during passage. The maximal inhibition by B404 and other MAbs were significantly decreased against a recombinant virus with a gp41 truncation compared with the parental SIVmac316. This indicates that the gp41 truncation was associated with resistance to antibody-mediated neutralization. The infectivities of the recombinant virus with the gp41 truncation were 7,900-, 1,000-, and 140-fold higher than those of SIVmac316 in PM1, PM1/CCR5, and TZM-bl cells, respectively. Immunoblotting analysis revealed that the gp41 truncation enhanced the incorporation of Env into virions. The effect of the gp41 truncation on infectivity was not obvious in the HSC-F macaque cell line, although the resistance of viruses harboring the gp41 truncation to neutralization was maintained. These results suggest that viruses with a truncated gp41 cytoplasmic tail were selected by increased infectivity in human cells and by acquiring resistance to neutralizing antibody.

Keywords: SIV, gp41, truncation, infectivity, resistance, neutralization, antibody

INTRODUCTION

The RV144 trial demonstrated 31% vaccine efficacy for preventing human immunodeficiency virus type 1 (HIV-1) infection (Rerks-Ngarm et al., 2009). Antibodies against the HIV-1, particularly against the V1/V2 loops, correlate inversely with infection risk (Haynes et al., 2012). Further recent isolation of monoclonal antibodies (MAbs) that neutralize a broad range of HIV-1 strains suggest the possibility for developing a vaccine that can induce cross-neutralizing antibodies effective for various HIV-1 strains (Kwong and Mascola, 2012). Although non-human primate models of simian immunodeficiency virus (SIV) infection can facilitate the evaluation of immunogens, epitopes and immune correlates, no potent and broad neutralizing MAb against SIV had been available.

To understand the mechanisms involved in neutralization of infectivity by antibodies in an SIV model, we recently isolated MAb B404 from a SIVsmH635FC-infected rhesus macaque, which potently and broadly neutralizes various SIV strains, such as SIVsmE543-3, SIVsmE660 and the neutralization-resistant variants, genetically diverse SIVmac316, and highly neutralization-resistant SIVmac239 (Kuwata et al., 2011). The B404 epitope, which comprises the V3 and V4 loops of Env and is intensely exposed by ligation of Env to CD4, is the target for potent and broad neutralization of SIV (Kuwata et al., 2013). Vigorous induction of B404-like neutralizing antibodies using the specific VH3 gene with a long complementarity-determining region 3 loop and λ light chain was observed in four SIVsmH635FC-infected macaques. The B404-resistant variants were induced by passaging viruses in the presence of increasing concentrations of B404. Genetical analysis of the gp120 region of B404-resistant variants revealed that the mutations in the C2 region of Env were important for the resistance to antibody-mediated neutralization (Kuwata et al., 2013).

In the present study, we further analyzed B404-resistant variants and determined the precise region responsible for the resistance to antibody-mediated neutralization. Genetic analysis of viruses during passage in the presence of B404 as well as phenotypic analysis using recombinant viruses revealed that a truncation of the gp41 cytoplasmic tail was the primary step leading to escape from neutralization.

MATERIALS AND METHODS

CELLS

PM1 (Lusso et al., 1995), PM1/CCR5 (Yusa et al., 2005), and HSC-F (Akari et al., 1999) cells were maintained in Roswell Park Memorial Institute (RPMI) 1640 medium containing 10% fetal bovine serum (FBS). TZM-bl (Platt et al., 1998; Derdeyn et al., 2000; Wei et al., 2002; Takeuchi et al., 2008) and 293T (DuBridge et al., 1987) cells were maintained in Dulbecco's modified Eagle's medium containing 10% FBS.

GENETIC ANALYSIS OF B404-RESISTANT VARIANTS

The induction of variants resistant to Fab-B404 (Kuwata et al., 2011) from SIVmac316 (Mori et al., 1992) harboring full-length gp41 was performed as described previously (Yoshimura et al., 2006; Hatada et al., 2010; Kuwata et al., 2013). Briefly, 5,000 $TCID_{50}$ (50% tissue culture infectious dose) SIVmac316 was incubated with 5 ng/ml Fab-B404 for 30 min at 37°C. Then, 5×10^4 PM1/CCR5 cells were added to the virus–Fab mixture. After incubation for 5 h, cells were washed with phosphate-buffered saline (PBS) and resuspended in RPMI 1640 supplemented with 10% FBS without Fab-B404. The culture supernatant was harvested 7 days later and used to infect fresh PM1/CCR5 cells for the next round of culture in the presence of increasing concentrations of Fab-B404. Proviral DNA samples were extracted from cells using a QIAamp DNA Blood Mini Kit (QIAGEN, Hilden, Germany) after 8, 17, 20, 23, and 26 passages as well as from P26C cells obtained after 26 passages in the absence of Fab-B404. The gp120 region was amplified using Platinum Taq DNA Polymerase High Fidelity (Invitrogen, Carlsbad, CA, USA) with primers SEnv-F (5′-ATG GGA TGT CTT GGG AAT CAG C-3′) and SER1 (5′-CCA AGA ACC CTA GCA CAA AGA CCC-3′). The whole *env* gene was amplified with primers SRev-F (5′-GGT TTG GGA ATA TGC TAT GAG-3′) and SEnv-R (5′-CCT ACT AAG TCA TCA TCT T-3′). The polymerase chain reaction (PCR) products were cloned using a TA cloning kit (Invitrogen), and subjected to sequencing. Nucleotide sequences were aligned and analyzed phylogenetically using Molecular Evolutionary Genetics Analysis version 5 (MEGA5) (Tamura et al., 2011).

CONSTRUCTION OF INFECTIOUS MOLECULAR CLONES WITH THE Env REGION FROM B404-RESISTANT VARIANTS

One of the clones from passage 26, P26B404 clone 26, was selected for construction of recombinant viruses, because this clone had mutations typical of the major population of P26B404 variants. Infectious molecular clones SS, SN, and NS were generated by replacing fragments *Sph*I–*Sac*I [nucleotides (nt) 6,446–9,226], *Sph*I–*Nhe*I (nt 6,446–8,742), and *Nhe*I–*Sac*I (nt 8,742–9,226) with the corresponding regions of SIVmac316, respectively. Mutants F277V and N295S, which have point mutations at amino acid residues 277 and 295 of Env, respectively, were constructed by PCR mutagenesis using the SIVmac316 plasmid as template. The changes from phenylalanine (TTC) to valine (GTC) in F277V and asparagine (AAT) to serine (AGT) in N295S were introduced using primers F277VFw (5′-TTG GTT TGG CGT CAA TGG TAC TAG GGC-3′), F277VRv (5′-GTA CCA TTG ACG CCA AAC CAA G-3′), N295SFw (5′-GGC AAT AGT AGT AGA ACC ATA ATT AG-3′), and N295SRv (5′-AAT TAT GGT TCT ACT ACT ATT GCC-3′). Mutant and parental SIVmac316 plasmids were transfected into 293T cells using X-tremeGENE 9 DNA Transfection Reagent (Roche Molecular Biochemicals, Mannheim, Germany). After 2 days, the supernatants containing viruses were filtered (0.45 μm) and stored at −80°C.

ANALYSIS OF VIRAL INFECTIVITY

For determination of $TCID_{50}$ in PM1 and PM1/CCR5 cells, 5×10^4 cells in 50 μl were inoculated with 50 μl serially diluted virus stocks in a 96-well plate and cultured for 2 weeks. Virus replication was judged by observation of cytopathic effects (CPE) by light microscopy. The $TCID_{50}$ in TZM-bl cells was determined by measuring luciferase activities. Briefly, 100 μl medium, 50 μl serially diluted virus stock, and 50 μl 1×10^4 cells containing 37.5 μg/ml diethylaminoethyl (DEAE) dextran were added to the wells of a 96-well plate. The plate was then incubated at 37°C for 2 days. After washing with PBS, cells were lysed with 30 μl cell lysing buffer (Promega, Madison, WI, USA) for 15 min at room temperature (RT) and then 10 μl of cell lysate was transferred to a 96-well white solid plate (Coster, Cambridge, MA, USA). Luciferase activity was measured using a Centro XS3 LB960 microplate luminometer (Berthold Technologies, Bad Wildbad, Germany) and a luciferase assay system (Promega). The $TCID_{50}$ was calculated according to the formula of Reed and Muench (1938).

Infectivity of viruses in PM1, PM1/CCR5, and HSC-F cells was evaluated by detecting infected cells using flow cytometry as described previously (Kuwata et al., 2011). Briefly, PM1 and PM1/CCR5 cells were adjusted to 1×10^6 cells/ml and HSC-F cells were adjusted to 5×10^6 cells/ml. Aliquots of 100 μl cells per well in a 24-well plate were inoculated with 100 μl of diluted virus stocks. After incubation for 6 h, 800 μl fresh medium was added to wells. One-half of the cells in each well were collected at 4, 7, and 10 days post-inoculation. Cells were washed with PBS and fixed with IC Fixation Buffer (eBioscience, San Diego, CA, USA). After washing with Permeabilization Buffer (eBioscience) twice, the cells were intracellularly stained with 4 μg/ml (50 μl) anti-p27 Fab, B450 (Kuwata et al., 2011) by incubation for 20 min at RT. The cells were then incubated with 50 μl anti-HA antibody (1:200; 3F10, Roche Molecular Biochemicals) for 20 min at RT followed by incubation with 50 μl of anti-rat-FITC (1:500; Santa Cruz Biotechnology, Santa Cruz, CA, USA) for 20 min at RT. The stained cells were analyzed using a FACSCalibur (BD Biosciences, Franklin Lakes, NJ, USA). Frequencies of infected cells were determined by comparison with an uninfected control. Data analysis was performed using FlowJo (TreeStar, San Carlos, CA, USA).

All infectivity experiments were performed at least twice and the representative results are shown.

ANALYSIS OF NEUTRALIZING ACTIVITIES

The Fab clones B404 and K8, isolated from an SIV-infected macaque (Kuwata et al., 2011), and murine MAb M318T (Matsumi et al., 1995) were used to examine the sensitivity of viruses to antibody-mediated neutralization in TZM-bl cells as described previously (Kuwata et al., 2011). Briefly, 100 μl serially diluted antibodies in duplicate were incubated with 200 $TCID_{50}$ (50 μl) of virus in a 96-well plate. After incubation for 1 h at 37°C, 100 μl

of 1×10^5 TZM-bl cells/ml containing 37.5 μg/ml DEAE dextran were added. After incubation for 2 days, luciferase activities were measured as described above for the analysis of viral infectivity. The 50% inhibitory concentrations (IC_{50}) and maximal percent of inhibition (MPI) were calculated from the average values by non-linear regression using Prism5 (GraphPad Software, San Diego, CA, USA).

Sensitivity to neutralization by B404 in macaque cells was analyzed using HSC-F cells, a cynomolgus macaque cell line immortalized by infection with *Herpesvirus saimiri* (Akari et al., 1999). Fab-B404 was serially diluted and 50 μl aliquots were mixed with 50 μl undiluted or 10-fold diluted virus in a 96-well plate. After 1 h incubation at 37°C, 2×10^5 cells in 100 μl were added to each well and cultured for 1 day. The infected cells were washed twice with PBS, resuspended in 200 μl fresh medium, and cultured in a new 96-well plate. Viral infection was examined 4 days post-inoculation by intracellular staining of p27, as described above for the analysis of viral infectivity. Infectivity was determined in duplicate and the average value was used for the analysis of neutralization.

All neutralizing assays were performed at least twice and the representative results are shown.

WESTERN BLOTTING ANALYSIS OF VIRAL PROTEINS

Cells and supernatants were collected from six-well plate 2 days after transfection of 293T cells with infectious molecular clones, as previously described (Yuste et al., 2005). Supernatants were filtered (0.45 μm) and clarified by centrifugation for 10 min at 3,000 rpm. The clarified supernatants were centrifuged at 13,200 rpm for 90 min at 4°C, and the viral pellets were resuspended in 1 ml PBS and centrifuged again. Pellets were then dissolved in 80 μl sample buffer [62.5 mM Tris–HCl, pH 6.8, 2% sodium dodecyl sulfate (SDS), 25% glycerol, 5% 2-mercaptoethanol, 0.01% bromophenol blue]. Cells were washed with PBS and lysed in 300 μl sample buffer. Samples of virions and cell lysates were boiled for 5 min, and the proteins were separated by SDS-polyacrylamide gel electrophoresis using SuperSep Ace 5–20% (Wako Pure Chemical Industries, Osaka, Japan). Proteins were transferred to an Immun-Blot PVDF Membrane (Bio-Rad Laboratories, Hercules, CA, USA). The membrane was blocked with 5% skim milk TBS-T (Tris-buffered saline containing 0.1% Tween 20) for 1 h at RT, and then washed three times with TBS-T. For the detection of gp120, the membrane was incubated overnight at 4°C with 1 μg/ml M318T (Matsumi et al., 1995) in 5% skim milk TBS-T. After washing three times with TBS-T, the membrane was incubated with anti-mouse immunoglobulin G (IgG) peroxidase (1:4,000, Santa Cruz Biotechnology) for 1 h at RT. The membrane was washed three times with TBS-T and once with TBS, and then TMB solution (KPL, Gaithersburg, MD, USA) was added to develop color. Viral proteins gp41 and p26 were similarly examined using crude supernatants from bacterial culture producing B408 and B450 (Kuwata et al., 2011), which were mixed with the same amount of 5% skim milk TBS-T. The membrane was incubated with anti-HA-HRP antibody (1:1,000; Roche Molecular Biochemicals) and Chemi-Lumi One L (Nacalai Tesque, Kyoto, Japan), and viral proteins were visualized using ImageQuant LAS 4000 (GE Healthcare, Piscataway, NJ, USA)

RESULTS

EVOLUTION OF VIRUSES DURING PASSAGE UNDER THE PRESSURE OF Fab-B404

To select for variants resistant to MAb B404, an antibody that targets a conformational epitope comprising the gp120 V3 and V4 loops, we passaged SIVmac316 that possesses a full-length gp41 in PM1/CCR5 cells in the presence of increasing concentrations of Fab-B404. The virus recovered at passage 26 (P26B404) was resistant to neutralization by B404 (V3/V4) and other antibodies, MAbs K8 (CD4i) and M318T (V2), that target epitopes other than that recognized by B404 (Kuwata et al., 2013). The region covering the whole *env* gene were amplified by PCR and cloned from viruses at passage 8, 17, 20, 23, and 26. The nucleotide sequences were phylogenetically analyzed to show the evolution of B404-resistant variants (**Figure 1**). The first major mutation was a change from glutamine (CAG) to a stop codon (TAG) at 733rd amino acid residue of Env. The Q733stop substitution in the gp41 cytoplasmic domain was observed in 12 of 14 clones at passage 8 and in all clones thereafter. Another stop codon (W782stop) was the second

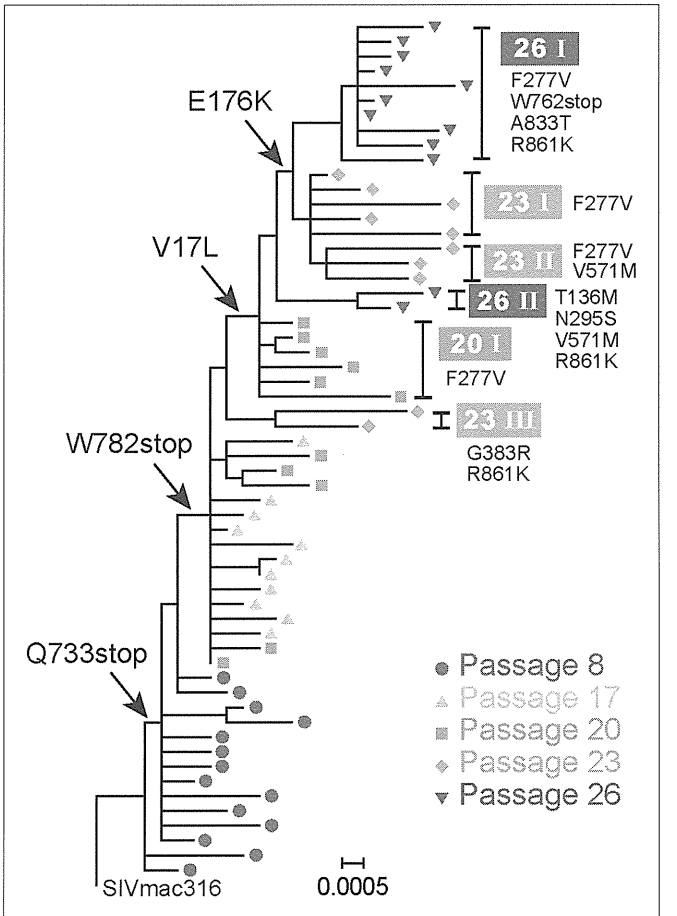

FIGURE 1 | Evolution of B404-resistant variants. Nucleotide sequences of the *env* gene, which were derived from proviruses at passages 8, 17, 20, 23, and 26, were phylogenetically analyzed using MEGA5. Arrows indicate major substitutions as follows: Q733stop, W782stop, V17L, and E176K. Clones with representative amino acid substitutions were separated into groups, which are shown on the right side along with the corresponding substitutions.

major mutation, which was detected after 17 passages. Substitutions V17L in the signal peptide and E176K in the V2 loop emerged after 20 and 23 passages, respectively, although the E176K substitution was also observed in P26C, control viruses after 26 passages in the absence of B404 (**Table 1**). In addition to these substitutions, most of clones acquired the F277V substitution in the late stage of evolution, except for one group at passage 26 which has the N295S substitution (see **Figure 1**, group 26II). Group 26II was clearly distinguished from group 26I by amino acid substitutions, such as T136M, N295S, and D571M/E (**Table 1**), suggesting two lineages of variants in P26B404.

These results demonstrated that the first step in acquiring resistance to B404 was the truncation of gp41. Although substitutions in gp120, represented by F277V, might contribute to the resistance to a high concentration of B404, 20 passages were required for the emergence of these substitutions.

Table 1 | Frequency* of amino acid substitutions in Env clones from B404-resistant variants after 26 passages.

Substitution	Region	P26B404		P26C
		I	II	
	gp120	**(*n* = 22)**	**(*n* = 8)**	**(*n* = 14)**
V17L	Signal peptide	**100%**	**100%**	0.0%
G62S	C1	0.0%	0.0%	21.4%
M67V/L/T	C1	4.5%	0.0%	21.4%
A68T	C1	0.0%	0.0%	**92.9%**
T136M	V1	4.5%	**87.5%**	0.0%
T137I	V1	0.0%	0.0%	14.3%
K141E/R	V1	0.0%	12.5%	7.1%
E176K	V2	**90.9%**	12.5%	35.7%
F277V	C2	**100%**	0.0%	0.0%
N295S	C2	0.0%	**100%**	0.0%
Q341H	V3	13.6%	12.5%	14.3%
D374N	C3	0.0%	0.0%	28.6%
K403R	V4	0.0%	12.5%	7.1%
W441R	C4	4.5%	0.0%	7.1%
	gp41	**(*n* = 10)**	**(*n* = 2)**	**(*n* = 7)**
F528S/L	Extracellular	20.0%	0.0%	0.0%
D571M/E	Extracellular	10.0%	**100%**	0.0%
Q733stop	Cytoplasmic	**100%**	**100%**	0.0%
W762stop	Cytoplasmic	**100%**	0.0%	0.0%
W782stop	Cytoplasmic	**100%**	0.0%	0.0%
A833T	Cytoplasmic	**90.0%**	0.0%	0.0%
R839K	Cytoplasmic	0.0%	0.0%	**57.1%**
R861K	Cytoplasmic	**100%**	**100%**	0.0%

Percentages of substitutions in populations P26B404 and P26C, which were obtained after 26 passages in the presence and absence of B404, respectively, are shown. The P26B404 population is separated into two subpopulations according to the phylogenetic analysis in **Figure 1. All the substitutions that are observed in more than one clone are shown here. Boldface indicates substitutions dominant (>50%) in each population. The numbers of clones analyzed for the gp120 and gp41 regions are shown in parentheses.*

TRUNCATION OF gp41 CONFERRED RESISTANCE TO ANTIBODY-MEDIATED NEUTRALIZATION

To analyze effect of substitutions in B404-resistant variants on resistance to neutralization, recombinant viruses were constructed (**Figure 2**). The *env* region of SIVmac316 was replaced by that of P26B404 clone 26, which had substitutions typical to the P26I group. The resultant molecular clones SS, SN, and NS had substitutions in the entire *env* region, gp120 and gp41 from P26B404I, respectively. SS and NS were predicted to have a truncated gp41 with no other mutation in gp41, because the Q733stop substitution was the first substitution in gp41. Point mutants with substitutions F277V and N295S, which were representative mutations at late passages, were also constructed by PCR mutagenesis.

These mutant viruses were examined for their sensitivity to neutralization by three MAbs B404 (V3/V4 conformational), K8 (CD4i), and M318T (V2). The neutralization of SS that contain the entire *env* region from P26B404I was similar to those of P26B404, indicating that the *env* region is responsible for the

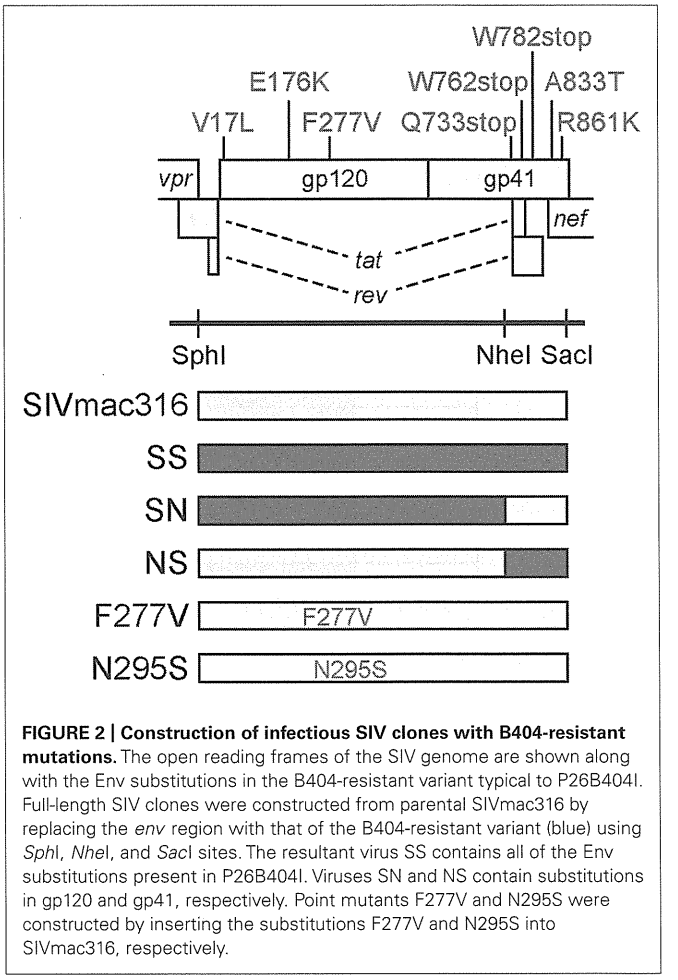

FIGURE 2 | Construction of infectious SIV clones with B404-resistant mutations. The open reading frames of the SIV genome are shown along with the Env substitutions in the B404-resistant variant typical to P26B404I. Full-length SIV clones were constructed from parental SIVmac316 by replacing the *env* region with that of the B404-resistant variant (blue) using *Sph*I, *Nhe*I, and *Sac*I sites. The resultant virus SS contains all of the Env substitutions present in P26B404I. Viruses SN and NS contain substitutions in gp120 and gp41, respectively. Point mutants F277V and N295S were constructed by inserting the substitutions F277V and N295S into SIVmac316, respectively.

resistance to neutralization (**Figure 3A**). Recombinants SN and NS, which have substitutions in gp120 and gp41 from P26B404I, respectively, showed varying degrees of resistance. The IC_{50} values of SN and NS against B404 were intermediates between the parental SIVmac316 and the neutralization-resistant P26B404. Maximal inhibition reached a plateau at 73.8, 82.3, and 81.9% in SS, NS, and P26B404, respectively, but the MPI value of SN (94.9%) was close to that of SIVmac316 (100%; **Figure 3B**). Neutralization resistance to anti-CD4i MAb K8 was characterized by decreases in the IC_{50} value of SN and the MPI of NS. Neutralization by anti-V2 MAb M318T was even enhanced in SN, although NS showed the resistance comparable to those of SS and P26B404. The decreases in MPI values were commonly observed for the neutralization of NS by the three MAbs (**Figure 3B**). Resistance to neutralization was not significantly detected by the point mutants F277V and N295S, except for the neutralization of F277V by K8 (4.3-fold decrease of IC_{50} value). These results indicated that the entire *env* region, including substitutions in both gp120 and gp41, was responsible for the full-resistance of P26B404 to neutralization. The decrease of MPI values for NS suggested that truncation of gp41 by the Q733stop substitution, the first major substitution in viral evolution, was important to escape from the neutralizing antibodies.

INCREASED INFECTIVITY FOR HUMAN CELLS BY SIV WITH A TRUNCATED gp41

Truncation of gp41 in SIV is associated with the adaptation to human cells (Hirsch et al., 1989; Kodama et al., 1989), which may partially contribute to neutralization resistance (Yuste et al., 2005). To explore the mechanism of neutralization resistance of P26B404, the infectivity of recombinant viruses was analyzed by determining the $TCID_{50}$ values of virus stocks prepared by transfection of 293T cells (**Table 2**). The $TCID_{50}$ values in all the human cells tested were significantly higher for SS and NS viruses with truncated gp41 than

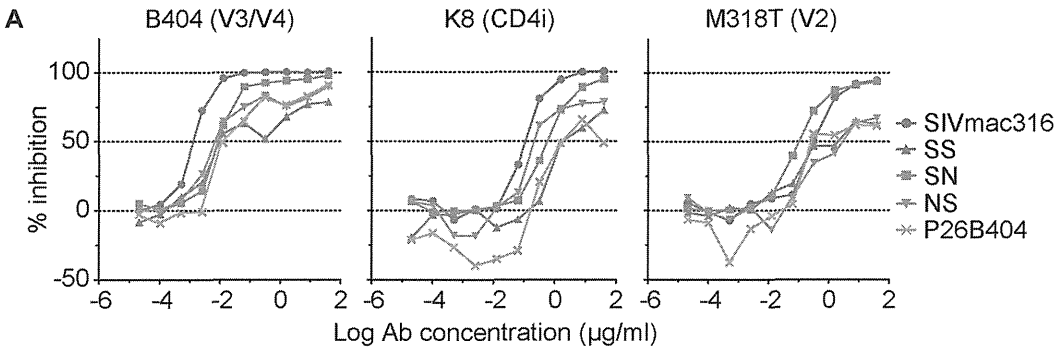

B

Neutralization profile of mutant viruses

Virus	B404 (V3/V4)		K8 (CD4i)		M318T (V2)	
	IC_{50}	MPI	IC_{50}	MPI	IC_{50}	MPI
SIVmac316	1.3E-03 (1.0)	100 (0.0)	1.1E-01 (1.0)	99.0 (0.0)	3.3E-01 (1.0)	94.3 (0.0)
SS	1.9E-02 (14.5)	73.8 (-26.2)	1.8E+00 (16.3)	67.9 (-31.1)	9.4E-01 (2.8)	65.5 (-28.8)
SN	9.1E-03 (6.8)	94.9 (-5.1)	5.9E-01 (5.3)	94.7 (-4.4)	1.0E-01 (0.3)	92.5 (-1.8)
NS	6.8E-03 (5.1)	82.3 (-17.7)	2.1E-01 (1.9)	77.0 (-22.0)	1.7E+00 (5.2)	67.6 (-26.7)
F277V	3.8E-03 (2.8)	100 (0.0)	4.8E-01 (4.3)	99.6 (0.5)	3.0E-01 (0.9)	94.8 (0.5)
N295S	2.3E-03 (1.7)	99.6 (-0.4)	1.4E-01 (1.2)	99.9 (0.8)	3.1E-01 (0.9)	97.0 (2.7)
P26B404	1.7E-02 (12.5)	81.9 (-18.1)	8.2E-01 (7.3)	54.6 (-44.5)	2.5E-01 (0.8)	60.0 (-34.3)

Fold change of IC_{50}	% change of MPI
> 10	< -20
3-10	-10- to -20
< 3	> -10

FIGURE 3 | Sensitivities of viruses with B404-resistant mutations to neutralization by MAbs. (A) Sensitivities of mutant viruses SS, SN, and NS to neutralization by MAbs Fab-B404 (anti-V3/V4), Fab-K8 (anti-CD4i), and M318T (anti-V2) are shown. Neutralization of parental SIVmac316 and B404-resistant P26B404 is also shown as controls sensitive and resistant to neutralization, respectively. **(B)** The sensitivities to neutralization are represented by values for IC_{50} (μg/ml) and MPI (%). Viruses were examined for their sensitivities to neutralization by MAbs Fab-B404, Fab-K8, and M318T in TZM-bl cells. The IC_{50} and MPI values were determined using Prism 5. The fold-change of IC_{50} was calculated by dividing the IC_{50} value by that of the parental SIVmac316. Percent change of MPI was calculated by subtracting the MPI value from that of SIVmac316. These changes are shown in parentheses and significant changes are indicated by magenta (IC_{50}: >10; MPI: < −20) and orange (IC_{50}: 3–10; MPI: −20 to −10) highlighting.

parental SIVmac316 and SN, in which gp41 is intact. In particular, NS showed a striking increase in $TCID_{50}$ values, which were 7,100-, 1,000-, and 140-fold higher than those of parental SIVmac316 in PM1, PM1/CCR5, and TZM-bl cells, respectively. These results indicate that truncation of gp41 caused by the Q733stop substitution increases viral infectivity for human cells.

To compare viral infectivity in human and macaque cells, viral infection was monitored after inoculation of PM1 and PM1/CCR5 human cells and the HSC-F cynomolgus macaque cell line with varying dilutions of virus stocks (**Figure 4**). Consistent with the $TCID_{50}$ analysis, a higher frequency of infected cells was detected earlier in PM1 and PM1/CCR5 cells inoculated with NS than the parental SIVmac316. In contrast, SN showed decreased infectivity in PM1 and PM1/CCR5 cells, apparently because PM1 cells were not infected by a 1,000-fold diluted SN stock. Although the $TCID_{50}$ values of SS were much higher than those of SIVmac316, the replication kinetics of SS were similar to those of SIVmac316 in PM1 and PM1/CCR5 cells. These results suggest that gp41 truncation increases infectivity for human cells and that the substitutions in gp120 of P26B404I are associated with slow and poor replication compared with that of SIVmac316.

Infectivity for macaque cells was more significantly affected than that for human cells by the substitutions in gp120 of P26B404I (**Figure 4**, lower panels). Infected cells were detected in HSC-F cells inoculated with 1,000-fold diluted virus stocks of SIVmac316 and NS, but viral infection in HSC-F cells was limited to a low frequency even by inoculation with 10-fold diluted virus stocks of SS and SN. Truncation of gp41 did not significantly affect replication in HSC-F macaque cells, although truncation of gp41 was disadvantageous for replication in primary T cell cultures from macaques (Hirsch et al., 1989; Kodama et al., 1989).

These results demonstrate that gp41 truncation strikingly increases infectivity for human cells, but not for macaque cells, and that the substitutions in gp120 decrease infectivity in human and macaque cells. Truncation of gp41, which conferred extremely high infectivity for PM1/CCR5 cells, may be the first step to escape from neutralization and the substitutions in gp120 may be the second step to replicate in the presence of high concentration of B404.

Table 2 | Infectivity* of viruses with substitutions from P26B404.

Viruses	PM1	PM1/CCR5	TZM-bl
SIVmac316	4.2E+02 (1.0)	1.4E+03 (1.0)	9.6E+04 (1.0)
SS	2.9E+05 (710)	4.7E+05 (350)	6.3E+06 (66)
SN	2.0E+03 (4.8)	8.4E+03 (6.2)	2.9E+05 (3.1)
NS	2.9E+06 (7,100)	1.4E+06 (1,000)	1.4E+07 (140)

**Infectivity is shown by the $TCID_{50}$/ml values of the viruses, which were prepared by transfection of 293T cells, in PM1, PM1/CCR5, and TZM-bl cells. The fold-change, which was calculated by dividing the mutant $TCID_{50}$/ml value by that of the parental SIVmac316, is shown in the parentheses.*

INCREASED INCORPORATION OF Env INTO VIRIONS IN SIV WITH TRUNCATED gp41

Incorporation of Env into virions was examined using these recombinant viruses, because increased infectivity by gp41 truncation was suggested to be associated with the Env content of virions (Manrique et al., 2001; Zhu et al., 2003, 2006; Yuste et al., 2004, 2005). Analysis of viral proteins in cells and supernatants from transfected 293T cells revealed that incorporation of Env into virions was significantly high in SS and NS viruses with the Q733stop substitution (**Figure 5**). MAb to gp120 showed a higher amount

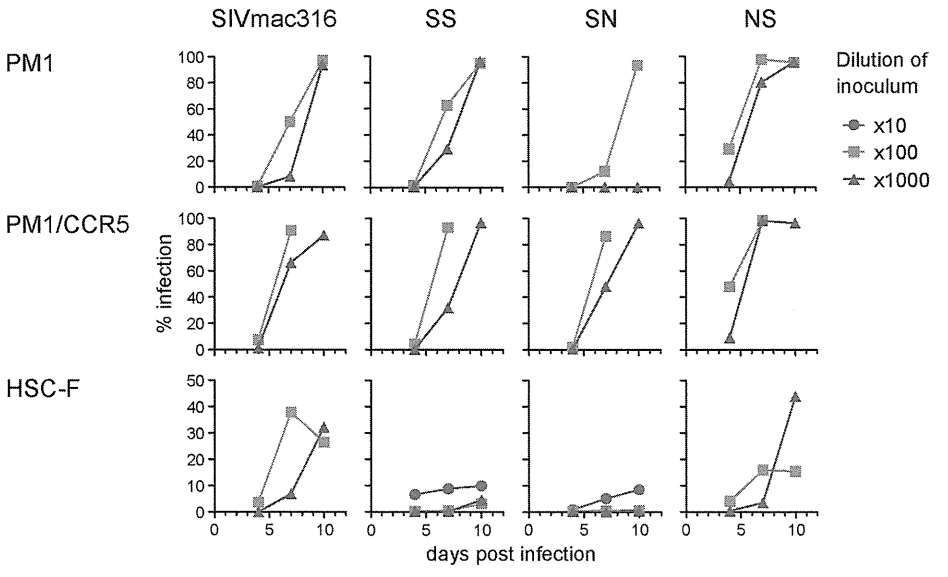

FIGURE 4 | Replication of B404-resistant viruses in human and macaque cells. Frequencies of infected cells at 4, 7, and 10 days post-infection are shown. PM1 and PM1/CCR5 human T cells and HSC-F cynomolgus macaque T cells were infected with the various dilutions of SIVmac316, SS, SN, and NS. Infected cells were detected using flow cytometry after intracellular staining by B450 (anti-p27 Fab).

of gp120 and gp160 in virions from SS and NS than those from SN and the parental SIVmac316, although the production of Env proteins in the transfected cells was at the same level among all the viruses (**Figure 5A**). MAb to gp41 also demonstrated that truncated gp41 was more abundant in virions compared with full-length gp41 (**Figure 5B**). Semi-quantification by densitometric scanning of gp41 and p26 images suggested that the levels of gp41 amount per virion in SS and NS were 12- and 44-fold higher than that of SIVmac316, respectively, after adjusting virion numbers using the p26 amounts. In contrast to the increased amount of Env proteins in virions from viruses with truncated gp41, the level of Gag p27 in virions was low in SS and NS compared with those in SN and SIVmac316 (**Figure 5C**). This indicates that the Env content per virion, which was normalized by the amount of p27, was significantly high in viruses with truncated gp41. These results suggest that truncation of gp41 by the Q733stop substitution enhances incorporation of Env into virions.

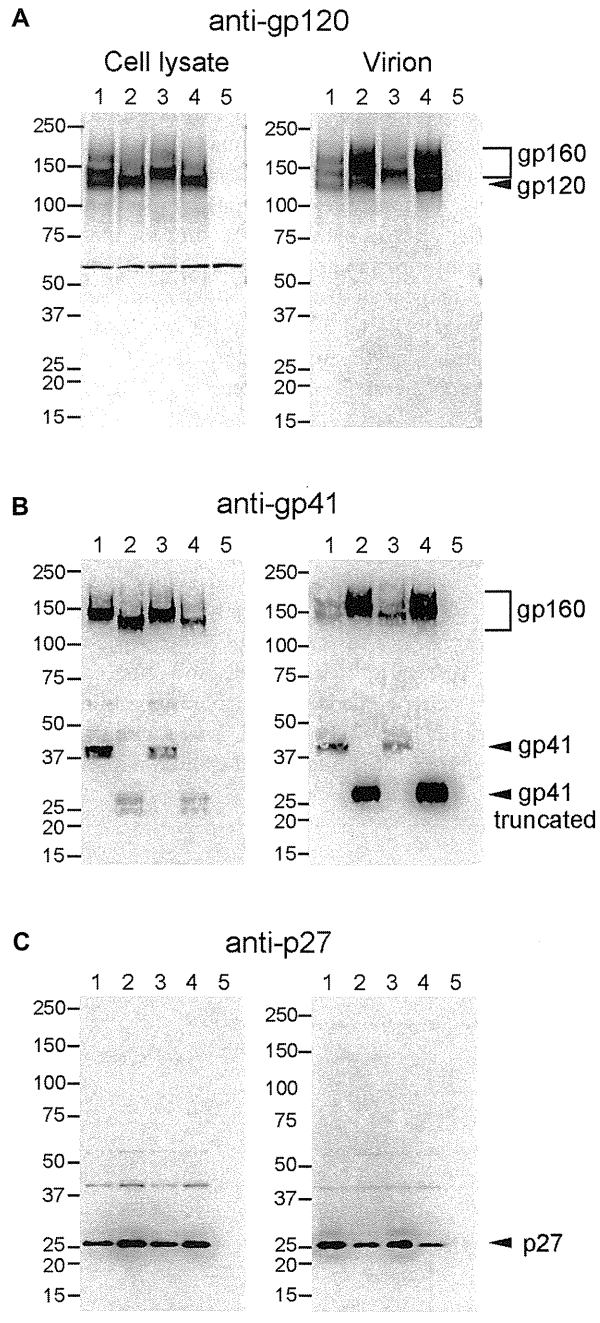

FIGURE 5 | Effect of B404-resistant mutations on the incorporation of Env into virions. Cell lysates (left panels) and virions (right panels) of SIVmac316 (lane 1), SS (lane 2), SN (lane 3), NS (lane 4), and mock-infected control (lane 5), which were prepared from transfected 293T cells, were analyzed by Western blotting. Viral proteins gp120 **(A)**, gp41 **(B)**, and p27 **(C)** were detected using MAbs M318T (anti-gp120 V2), B408 (anti-gp41 cluster I), and B450 (anti-p27), respectively.

NEUTRALIZATION RESISTANCE OF SIV WITH TRUNCATED gp41 IN MACAQUE CELLS

The analysis of infectivity of recombinant viruses suggested that the resistance to neutralization by truncation of gp41 might be due to adaptation to human cells. To examine this hypothesis, sensitivity to neutralization by B404 was determined in HSC-F macaque cells using SIVmac316 and NS, which showed similar infectivity for HSC-F cells (**Figure 4**). In flow cytometric analysis, infection in the presence or absence of B404 demonstrated that the high sensitivity of SIVmac316 and resistance of NS to neutralization were maintained in HSC-F cells (**Figure 6**). The frequency of infected cells decreased from 41.5% to the background level (2.03%) in inoculation with the undiluted stock of SIVmac316. In contrast, infection with NS, even with a 10-fold diluted virus stock, was significant in HSC-F cells in the presence of B404 (**Figure 6A**). Neutralization of NS in HSC-F cells was characterized by a decrease in maximal inhibition (**Figure 6B**), which was also observed in TZM-bl cells (**Figure 3A**). The magnitude of resistance of NS to B404 was greater when infection was performed using the undiluted stock compared with the 10-fold diluted stock, raising the possibility that B404 did not inhibit infection with a high titer of viruses. However, the resistance of NS was shown by infection with a low titer of NS, in which the frequency of infected cells in the absence of B404 (23.8%) was lower than infection with undiluted SIVmac316 (41.5%). Further, immunoblotting analysis revealed that the amount of virions was higher in the virus stock of SIVmac316 than that of NS (**Figure 5**).

These results indicate that gp41 truncation by the Q733stop substitution contributes to neutralization resistance of viruses in macaque cells. This suggests that the resistance to neutralization by truncation of gp41 is not due to the adaptation to human cells. The Q733stop substitution, the first major mutation during passages in the presence of B404, might be selected because it facilitates adaptation of virus to human cells and imparts resistance to antibody.

DISCUSSION

In the present study, truncation of the cytoplasmic tail of gp41, which was caused by the Q733stop substitution in Env, was the first major mutation detected during passage of SIV in the presence of the neutralizing antibody B404. Analysis of recombinant viruses suggested that the gp41 truncation was selected by their resistance to neutralizing antibody, which was characterized by the decrease of maximal inhibition compared with viruses with intact gp41, and

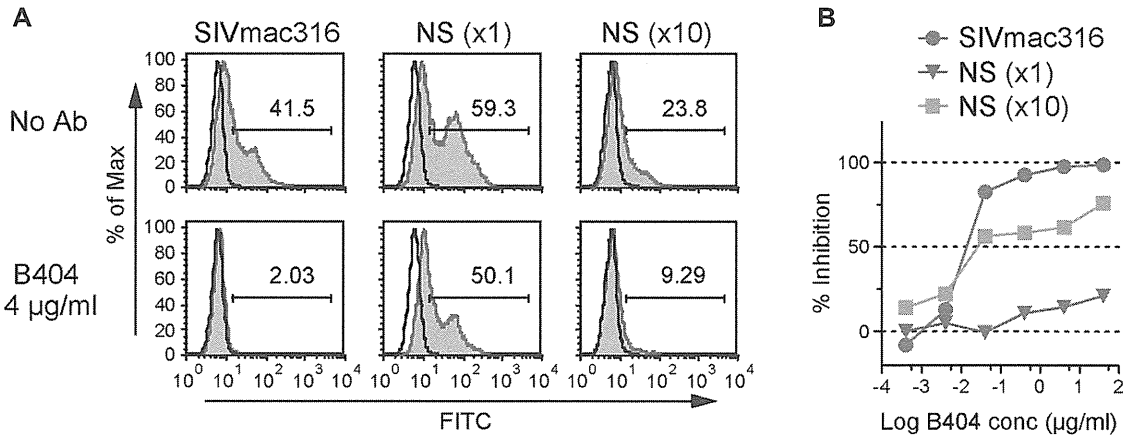

FIGURE 6 | Contribution of gp41 truncation to neutralization resistance in infection of macaque cells. (A) Infection of HSC-F cells in the presence (4 μg/ml) or absence of Fab-B404 is shown. HSC-F cells were inoculated with undiluted SIVmac316 and NS, and 10-fold diluted NS. Viral infection was monitored 4 days post-infection using flow cytometry after intracellular staining by B450 (anti-p27 Fab). **(B)** Neutralization of SIVmac316 and NS by B404 in HSC-F cells are shown. Percent inhibition was calculated by comparison with the infected culture in the absence of B404.

increased infectivity for human cells. The premature stop codon in the gp41 cytoplasmic region was frequently detected in SIV strains propagated in human cell culture *in vitro*, such as the original SIVmac316 clone, SIVmac1A11 and 17E-Fr (Hirsch et al., 1989; Kodama et al., 1989; Mori et al., 1992; Bonavia et al., 2005; Vzorov et al., 2005). The truncation of gp41 is considered as an adaptation of SIV to replication in human cell culture, because the premature stop codon rapidly reverted to express full-length gp41 after infection of rhesus primary cell culture *in vitro* and rhesus macaques *in vivo* (Hirsch et al., 1989; Kodama et al., 1989). Mutant viruses harboring the gp41 truncation showed increased infectivity for human cells, although the effects on infectivity varied depending on the SIV strain and the length of the gp41 truncation (Manrique et al., 2001; Yuste et al., 2004, 2005; Vzorov et al., 2005, 2007). The enhancement effect of gp41 truncation on incorporation of Env into virions, which were demonstrated by quantification of viral proteins in virions (Yuste et al., 2004) and electron tomography analysis of Env trimers on virions (Zhu et al., 2003, 2006), was partly associated with the increased infectivity caused by gp41 truncation (Manrique et al., 2001; Yuste et al., 2004, 2005). Because expression of Env on the cell surface is regulated by the cytoplasmic domain of gp41, truncation of gp41 may increase Env density on both cells and virions (LaBranche et al., 1995; Berlioz-Torrent et al., 1999; Postler and Desrosiers, 2013). Consistent with these studies, infectivity for human cells and Env incorporation into virions was enhanced by gp41 truncation in the present study. Although the mechanism responsible for increasing viral infectivity caused by gp41 truncation remains unclear, the high virion Env content may contribute to the efficient replication of viruses with truncated gp41 in human cells.

The effect of gp41 truncation on susceptibility to antibody-mediated neutralization is controversial, perhaps due to the SIV strains used for the analyses. Because most of prototypic SIV clones with truncated gp41 were macrophage-tropic, CD4-independent, and neutralization-sensitive (Mori et al., 1992; Bonavia et al., 2005; Vzorov et al., 2005), the truncation of gp41 was assumed responsible for the high sensitivity to neutralization. However, the resistance to neutralization by gp41 truncation was shown using the E767stop mutant of SIVmac316 (Yuste et al., 2005). This is consistent with our results using SIVmac316 harboring the Q733stop substitution, indicating that gp41 truncation contributes to resistance of SIVmac316 to neutralization. The increased infectivity of viruses with gp41 truncation in human cells may partially play a role in resistance by overcoming antibody-mediated neutralization via efficient attachment and entry of viruses to cells. However, we showed that gp41 truncation was also associated with neutralization resistance in macaque cells, in which gp41 truncation did not significantly affect infectivity. This suggests that the increased infectivity in human cells does not significantly affect the neutralization resistance of viruses with truncated gp41. As shown by provision of excess Env in trans, high Env content in virions may be critical for antibody-mediated neutralization (Yuste et al., 2005). Further studies will be required to understand the mechanism of resistance to neutralization conferred by gp41 truncation.

In the present study, we demonstrated that truncation of the cytoplasmic tail of gp41 contributes to resistance to antibody-mediated neutralization. Although non-human primate models of SIV infection are commonly used to estimate vaccine efficacy, the lack of broadly neutralizing MAbs has hampered development of antibody-based vaccine candidates in an SIV-macaque model. The broadly neutralizing MAb B404, which neutralizes multiple, diverse SIV isolates (Kuwata et al., 2013), is a useful tool for understanding the mechanism of neutralization in an SIV-macaque model and will contribute to the development of HIV-1 vaccines.

ACKNOWLEDGMENTS

We thank Dr. Hirofumi Akari for providing HSC-F cells. TZM-bl cells were obtained from Dr. John C. Kappes, Dr. Xiaoyun Wu, and Tranzyme Inc. through the NIH AIDS Research and Reference Reagent Program, Division of AIDS, NIAID, NIH. This work

was supported by MEXT KAKENHI Grant Number 10839786, the Program of Founding Research Centres for Emerging and Re-emerging Infectious Diseases, the Global COE program Global Education and Research Centre Aiming at the Control of AIDS and a grant-in-aid for scientific research (C-24591484) from the Ministry of Education, Culture, Sport, Science and Technology, Japan and a grant from the Ministry of Health, Welfare and Labour of Japan (H24-AIDS-007).

REFERENCES

Akari, H., Nam, K. H., Mori, K., Otani, I., Shibata, H., Adachi, A., et al. (1999). Effects of SIVmac infection on peripheral blood CD4+CD8+ T lymphocytes in cynomolgus macaques. *Clin. Immunol.* 91, 321–329.

Berlioz-Torrent, C., Shacklett, B. L., Erdtmann, L., Delamarre, L., Bouchaert, I., Sonigo, P., et al. (1999). Interactions of the cytoplasmic domains of human and simian retroviral transmembrane proteins with components of the clathrin adaptor complexes modulate intracellular and cell surface expression of envelope glycoproteins. *J. Virol.* 73, 1350–1361.

Bonavia, A., Bullock, B. T., Gisselman, K. M., Margulies, B. J., and Clements, J. E. (2005). A single amino acid change and truncated TM are sufficient for simian immunodeficiency virus to enter cells using CCR5 in a CD4-independent pathway. *Virology* 341, 12–23.

Derdeyn, C. A., Decker, J. M., Sfakianos, J. N., Wu, X., O'Brien, W. A., Ratner, L., et al. (2000). Sensitivity of human immunodeficiency virus type 1 to the fusion inhibitor T-20 is modulated by coreceptor specificity defined by the V3 loop of gp120. *J. Virol.* 74, 8358–8367.

DuBridge, R. B., Tang, P., Hsia, H. C., Leong, P. M., Miller, J. H., and Calos, M. P. (1987). Analysis of mutation in human cells by using an Epstein–Barr virus shuttle system. *Mol. Cell. Biol.* 7, 379–387.

Hatada, M., Yoshimura, K., Harada, S., Kawanami, Y., Shibata, J., and Matsushita, S. (2010). Human immunodeficiency virus type 1 evasion of a neutralizing anti-V3 antibody involves acquisition of a potential glycosylation site in V2. *J. Gen. Virol.* 91, 1335–1345.

Haynes, B. F., Gilbert, P. B., Mcelrath, M. J., Zolla-Pazner, S., Tomaras, G. D., Alam, S. M., et al. (2012). Immune-correlates analysis of an HIV-1 vaccine efficacy trial. *N. Engl. J. Med.* 366, 1275–1286.

Hirsch, V. M., Edmondson, P., Murphey-Corb, M., Arbeille, B., Johnson, P. R., and Mullins, J. I. (1989). SIV adaptation to human cells. *Nature* 341, 573–574.

Kodama, T., Wooley, D. P., Naidu, Y. M., Kestler, H. W. III, Daniel, M. D., Li, Y., et al. (1989). Significance of premature stop codons in env of simian immunodeficiency virus. *J. Virol.* 63, 4709–4714.

Kuwata, T., Katsumata, Y., Takaki, K., Miura, T., and Igarashi, T. (2011). Isolation of potent neutralizing monoclonal antibodies from an SIV-Infected rhesus macaque by phage display. *AIDS Res. Hum. Retroviruses* 27, 487–500.

Kuwata, T., Takaki, K., Yoshimura, K., Enomoto, I., Wu, F., Ourmanov, I., et al. (2013). Conformational epitope consisting of the V3 and V4 loops as a target for potent and broad neutralization of simian immunodeficiency viruses. *J. Virol.* 87, 5424–5436.

Kwong, P. D., and Mascola, J. R. (2012). Human antibodies that neutralize HIV-1: identification, structures, and B cell ontogenies. *Immunity* 37, 412–425.

LaBranche, C. C., Sauter, M. M., Haggarty, B. S., Vance, P. J., Romano, J., Hart, T. K., et al. (1995). A single amino acid change in the cytoplasmic domain of the simian immunodeficiency virus transmembrane molecule increases envelope glycoprotein expression on infected cells. *J. Virol.* 69, 5217–5227.

Lusso, P., Cocchi, F., Balotta, C., Markham, P. D., Louie, A., Farci, P., et al. (1995). Growth of macrophage-tropic and primary human immunodeficiency virus type 1 (HIV-1) isolates in a unique CD4+ T-cell clone (PM1): failure to downregulate CD4 and to interfere with cell-line-tropic HIV-1. *J. Virol.* 69, 3712–3720.

Manrique, J. M., Celma, C. C., Affranchino, J. L., Hunter, E., and Gonzalez, S. A. (2001). Small variations in the length of the cytoplasmic domain of the simian immunodeficiency virus transmembrane protein drastically affect envelope incorporation and virus entry. *AIDS Res. Hum. Retroviruses* 17, 1615–1624.

Matsumi, S., Matsushita, S., Yoshimura, K., Javaherian, K., and Takatsuki, K. (1995). Neutralizing monoclonal antibody against a external envelope glycoprotein (gp110) of SIVmac251. *AIDS Res. Hum. Retroviruses* 11, 501–508.

Mori, K., Ringler, D. J., Kodama, T., and Desrosiers, R. C. (1992). Complex determinants of macrophage tropism in env of simian immunodeficiency virus. *J. Virol.* 66, 2067–2075.

Platt, E. J., Wehrly, K., Kuhmann, S. E., Chesebro, B., and Kabat, D. (1998). Effects of CCR5 and CD4 cell surface concentrations on infections by macrophagetropic isolates of human immunodeficiency virus type 1. *J. Virol.* 72, 2855–2864.

Postler, T. S., and Desrosiers, R. C. (2013). The tale of the long tail: the cytoplasmic domain of HIV-1 gp41. *J. Virol.* 87, 2–15.

Reed, L. J., and Muench, H. (1938). A simple method of estimating fifty per cent endpoints. *Am. J. Epidemiol.* 27, 493–497.

Rerks-Ngarm, S., Pitisuttithum, P., Nitayaphan, S., Kaewkungwal, J., Chiu, J., Paris, R., et al. (2009). Vaccination with ALVAC and AIDSVAX to prevent HIV-1 infection in Thailand. *N. Engl. J. Med.* 361, 2209–2220.

Takeuchi, Y., Mcclure, M. O., and Pizzato, M. (2008). Identification of gammaretroviruses constitutively released from cell lines used for human immunodeficiency virus research. *J. Virol.* 82, 12585–12588.

Tamura, K., Peterson, D., Peterson, N., Stecher, G., Nei, M., and Kumar, S. (2011). MEGA5: molecular evolutionary genetics analysis using maximum likelihood, evolutionary distance, and maximum parsimony methods. *Mol. Biol. Evol.* 28, 2731–2739.

Vzorov, A. N., Gernert, K. M., and Compans, R. W. (2005). Multiple domains of the SIV Env protein determine virus replication efficiency and neutralization sensitivity. *Virology* 332, 89–101.

Vzorov, A. N., Weidmann, A., Kozyr, N. L., Khaoustov, V., Yoffe, B., and Compans, R. W. (2007). Role of the long cytoplasmic domain of the SIV Env glycoprotein in early and late stages of infection. *Retrovirology* 4, 94.

Wei, X., Decker, J. M., Liu, H., Zhang, Z., Arani, R. B., Kilby, J. M., et al. (2002). Emergence of resistant human immunodeficiency virus type 1 in patients receiving fusion inhibitor (T-20) monotherapy. *Antimicrob. Agents Chemother.* 46, 1896–1905.

Yoshimura, K., Shibata, J., Kimura, T., Honda, A., Maeda, Y., Koito, A., et al. (2006). Resistance profile of a neutralizing anti-HIV monoclonal antibody, KD-247, that shows favourable synergism with anti-CCR5 inhibitors. *AIDS* 20, 2065–2073.

Yusa, K., Maeda, Y., Fujioka, A., Monde, K., and Harada, S. (2005). Isolation of TAK-779-resistant HIV-1 from an R5 HIV-1 GP120 V3 loop library. *J. Biol. Chem.* 280, 30083–30090.

Yuste, E., Johnson, W., Pavlakis, G. N., and Desrosiers, R. C. (2005). Virion envelope content, infectivity, and neutralization sensitivity of simian immunodeficiency virus. *J. Virol.* 79, 12455–12463.

Yuste, E., Reeves, J. D., Doms, R. W., and Desrosiers, R. C. (2004). Modulation of Env content in virions of simian immunodeficiency virus: correlation with cell surface expression and virion infectivity. *J. Virol.* 78, 6775–6785.

Zhu, P., Chertova, E., Bess, J., Lifson, J. D., Arthur, L. O., Liu, J., et al. (2003). Electron tomography analysis of envelope glycoprotein trimers on HIV and simian immunodeficiency virus virions. *Proc. Natl. Acad. Sci. U.S.A.* 100, 15812–15817.

Zhu, P., Liu, J., Bess, J., Chertova, E., Lifson, J. D., Grisé, H., et al. (2006). Distribution and three-dimensional structure of AIDS virus envelope spikes. *Nature* 441, 847–852.

Conflict of Interest Statement: The authors declare that the research was conducted in the absence of any commercial or financial relationships that could be construed as a potential conflict of interest.

Received: 22 March 2013; accepted: 25 April 2013; published online: 14 May 2013.

*Citation: Kuwata T, Takaki K, Enomoto I, Yoshimura K and Matsushita S (2013) Increased infectivity in human cells and resistance to antibody-mediated neutralization by truncation of the SIV gp41 cytoplasmic tail. Front. Microbiol. **4**:117. doi: 10.3389/fmicb.2013.00117*

This article was submitted to Frontiers in Virology, a specialty of Frontiers in Microbiology.

Bioorganic & Medicinal Chemistry 21 (2013) 7884–7889

Contents lists available at ScienceDirect

Bioorganic & Medicinal Chemistry

journal homepage: www.elsevier.com/locate/bmc

A CD4 mimic as an HIV entry inhibitor: Pharmacokinetics

Chie Hashimoto [a], Tetsuo Narumi [a], Hiroyuki Otsuki [b], Yuki Hirota [a], Hiroshi Arai [a], Kazuhisa Yoshimura [c,d], Shigeyoshi Harada [c,d], Nami Ohashi [a], Wataru Nomura [a], Tomoyuki Miura [b], Tatsuhiko Igarashi [b], Shuzo Matsushita [d], Hirokazu Tamamura [a,*]

[a] Institute of Biomaterials and Bioengineering, Tokyo Medical and Dental University, Chiyoda-ku, Tokyo 101-0062, Japan
[b] Institute for Virus Research, Kyoto University, Kyoto 606-8507, Japan
[c] AIDS Research Center, National Institute of Infectious Diseases, Shinjuku-ku, Tokyo 162-8640, Japan
[d] Center for AIDS Research, Kumamoto University, Kumamoto 860-0811, Japan

ARTICLE INFO

Article history:
Received 17 September 2013
Revised 5 October 2013
Accepted 5 October 2013
Available online 17 October 2013

Keywords:
CD4 mimic
HIV entry inhibitor
Intravenous administration
Pharmacokinetics

ABSTRACT

To date, several small molecules of CD4 mimics, which can suppress competitively the interaction between an HIV-1 envelope glycoprotein gp120 and a cellular surface protein CD4, have been reported as viral entry inhibitors. A lead compound **2** (YYA-021) with relatively high potency and low cytotoxicity has been identified previously by SAR studies. In the present study, the pharmacokinetics of the intravenous administration of compound **2** in rats and rhesus macaques is reported. The half-lives of compound **2** in blood in rats and rhesus macaques suggest that compound **2** shows wide tissue distribution and relatively high distribution volumes. A few hours after the injection, both plasma concentrations of compound **2** maintained micromolar levels, indicating it might have promise for intravenous administration when used combinatorially with anti-gp120 monoclonal antibodies.

1. Introduction

Several anti-HIV-1 drugs, including protease inhibitors and integrase inhibitors have been developed and have contributed to the highly active anti-retroviral therapy (HAART) used to treat AIDS.[1] Prevention of the HIV-1 infection of its target cells[1,2] is however a legitimate goal and the viral attachment process is an important target for the development of the drugs which could forestall such infection. The dynamic and supramolecular entry of human immunodeficiency virus type 1 (HIV-1) into target cells is initiated by the interaction of a viral envelope glycoprotein gp120 with the cell surface protein CD4.[3] Sequential binding of CD4 and a co-receptor (CCR5 or CXCR4) to gp120 can trigger a series of conformational rearrangements of gp41, a viral transmembrane glycoprotein mediating fusion between the viral and cellular membranes.[3–6] Control, especially of dynamic conformational changes of the envelope glycoproteins is a very attractive option.[7] To date, several small molecules that mimic CD4 have been developed as HIV-1 entry inhibitors, which competitively block the binding of gp120 to CD4[8] and the potential of these CD4 mimics has been explored (Fig. 1).[9–11] Furthermore, the interaction of CD4 mimics with a highly conserved pocket on gp120, designated as the 'Phe43 cavity', induces conformational changes in gp120,[12] a process which occurs with unfavorable binding entropy, and leads to a favorable enthalpy change similar to that caused by binding of the soluble CD4 binding to gp120. Thus, these unique properties render CD4 mimics valuable not only as entry inhibitors but also as 'envelope protein openers' and putatively, stimulants when combined with neutralizing antibodies.[13]

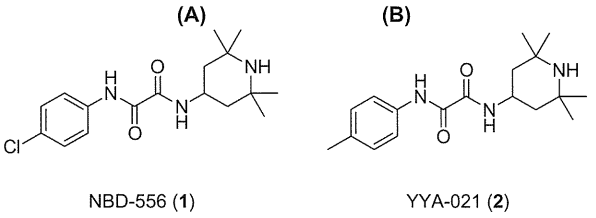

Figure 1. Structures of NBD-556 (**1**) and YYA-021 (**2**).

Through our SAR studies a lead compound YYA-021 (**2**) with relatively high potency and low cytotoxicity has been found,[11] although the original compound NBD-556 (**1**) had relatively high cytotoxicity. Pharmacokinetic (PK) studies were performed to assess the potential of compound **2** for clinical application and in addition, the possibility and the effectiveness of its use in combination with neutralization antibodies are discussed.

* Corresponding author. Tel.: +81 3 5280 8036; fax: +81 3 5280 8039.
E-mail address: tamamura.mr@tmd.ac.jp (H. Tamamura).

0968-0896/$ - see front matter © 2013 Elsevier Ltd. All rights reserved.
http://dx.doi.org/10.1016/j.bmc.2013.10.005

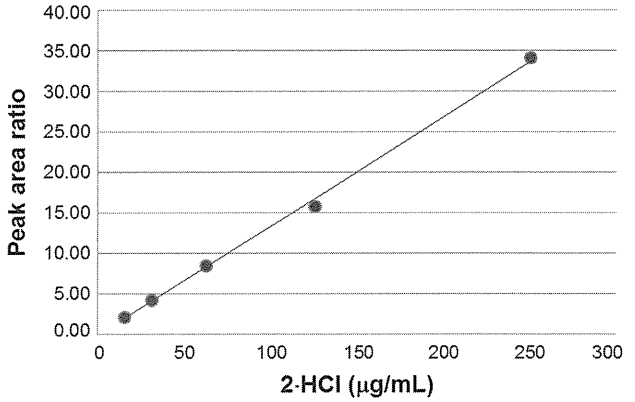

Figure 2. A calibration curve of compound **2·HCl** for calculating PK in rats.

2. Results and discussion

2.1. Calibration curve

Compound **2** was converted to its hydrochloride salt **2·HCl**, by treatment with 4 M HCl in dioxane. Standard solutions in saline of this HCl salt at concentrations over a range of 0–250 μg/mL were prepared and a calibration curve was constructed using the ratio of observed HPLC peak areas and concentrations of **2·HCl** to demonstrate the linearity shown in Figure 2.[14] The corresponding linear regression equation is $Y = 0.1345X$ ($R^2 = 0.9981$). Plasma concentrations of **2·HCl** were measured using this equation. The calibration curve shown in SD Figure S5C for the concentrations of compound **2** in plasma of a rhesus macaque was constructed using standard solutions of **2·HCl** in saline at concentrations over a range of 0–312.5 μg/mL. The linear regression equation in this case is $Y = 0.034X$ ($R^2 = 0.9927$). For adsorption of compound **2** by blood cells of a rhesus macaque, a calibration curve was constructed using standard solutions of **2·HCl** in saline at concentrations over a range of 0–950 μg/mL. The linear regression equation is $Y = 0.0553X$ ($R^2 = 0.9263$) and the curve is shown in SD Figure S7C.

2.2. Pharmacokinetics in rats

The primary stock solution of **2·HCl** was prepared in saline (2.5 mg/mL). Initially, the acute toxicity of compound **2** in rats was investigated to determine its maximum tolerated dose. The HCl salt, compound **2·HCl**, (0, 0.5, 1.0, 2.5 and 5.0 mg) was administered by tail vein injection into Jcl:SD rats (3 or 4 rats for each dose). Rats with the 5.0 mg administration showed a relatively low increase in the body weight although the intake amount of bait and water increased remarkably two weeks after administration, compared to the other rats (Supplementary data, SD Figs. S1 and S2). This observation suggested abnormalities such as renal and hepatic dysfunction and as a result, the maximum dose in rats of **2·HCl** was determined to be 2.5 mg.

Compound **2·HCl** (2.5 mg) in saline (1 mL) was administered at a level of 14 mg/kg by tail vein injection into Jcl:SD rats. Blood was collected from the tail vein into centrifugal blood collection tubes 15, 30, 45, 60, 120 and 240 min after administration of **2·HCl**. Plasma (50 μL) obtained from the blood sample was mixed with phenol in saline (final volume 60 μL) and centrifuged at 2000g for 3 min to remove any protein. The resultant supernatant was used in the analysis. A 50 μL aliquot of each filtrate was injected into HPLC by an autosampler. Compound **2** was detected in the HPLC analysis and was characterized by ESI-TOF-MS. The HPLC chart of the filtrate collected 30 min after administration of compound **2** is shown in Figure 3. Concentrations in blood of compound **2** after administration (15, 30, 45, 60, 120 and 240 min) were calculated using the calibration curve (SD Fig. S4) and plotted as shown in Figure 4.[15]

Using the data measured at 15, 30, 45, 60, 120 and 240 min, the half-life was calculated as 8.4 min by curve fitting with a one-compartment model based on GraphPad Prism Version 5.04 (GraphPad Software, CA, U.S.A). The initial concentration was calculated as 17.3 μg/mL. Compound **2** has a low molecular weight (317.4) and some level of hydrophobicity based on its structure, suggesting that the renal excretion is unlikely. At a dose of 2500 (μg)/initial concentration 17.3 (μg/mL), the volume of distribution was calculated as 145 mL, suggesting widespread tissue distribution of **2** as a result of its hydrophobicity.

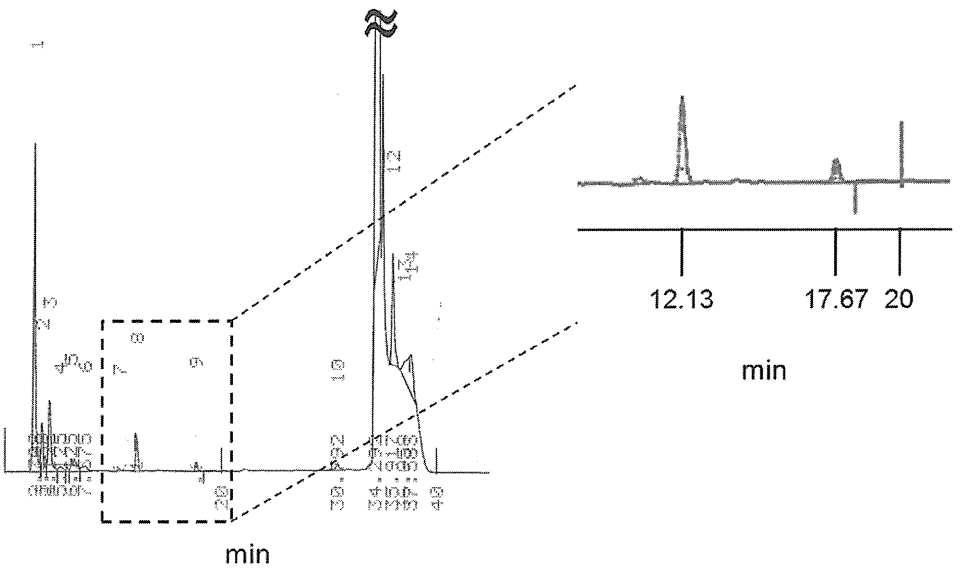

Figure 3. HPLC chart of rat plasma 30 min after intravenous administration of compound **2**. The plasma sample was eluted with a linear gradient of 20–35% CH_3CN (0.1% TFA, in 30 min). Peak 8 (retention time: 12.13 min) corresponds to the internal standard (phenol) and peak 9 (retention time: 17.67 min) corresponds to compound **2**.

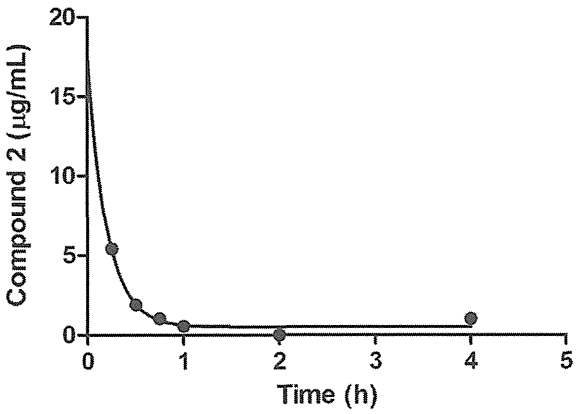

Figure 4. Plots of concentrations in rat blood of compound **2** after administration (15, 30, 45, 60, 120 and 240 min). Half-life is calculated as 0.141 h (8.4 min). The plasma of a representative rat was used for the analyses.

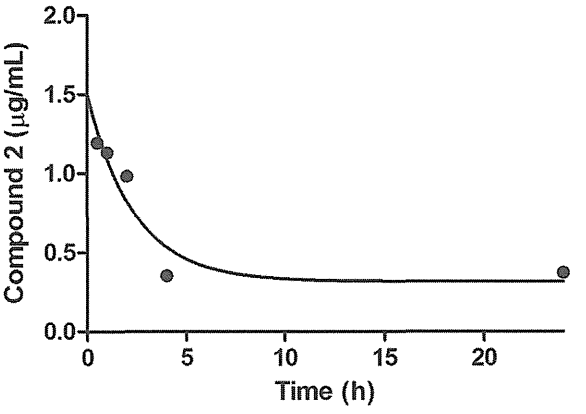

Figure 6. Plots of macaque blood concentrations of compound **2** after administration of **2·HCl** (0.5, 1, 2, 4 and 24 h). Half-life is calculated as 1.64 h (98.4 min). The plasma of a rhesus macaque was used for the analyses.

2.3. Pharmacokinetics in a rhesus macaque

The primary stock solution of the **2·HCl** was prepared in potassium-free phosphate-buffered saline (Na_2HPO_4 + NaH_2PO_4 + NaCl, pH 7.4) (2.4 mg/mL) to avoid hyperpotassemia and acidosis. Initially, the acute toxicity observed by treatment with **2·HCl** in a rhesus macaque was investigated to determine the maximum tolerated dose. **2·HCl** (14.1, 35.3 and 70.6 mg) was administered by cephalic vein injection into a rhesus macaque (one macaque for each dose). A macaque administered 70.6 mg, showed abnormalities such as mydriasis, prolonged PR interval in the electrocardiogram and bradycardia, while acute toxicity was not observed following the administration of **2·HCl** at levels up to 35.3 mg[16] and the maximum tolerated dose in a rhesus macaque was determined to be 35.3 mg (6.7 mg/kg). The macaque which had been administered 70.6 mg of **2·HCl** was treated by an emergency intervention with dobutamine (iv).

Compound **2·HCl** (70.6 mg) was intravenously administered at 13.4 mg/kg into a rhesus macaque. Blood (3.0 mL) was collected from cephalic vein 0, 0.5, 1, 2, 4 and 24 h after administration of the hydrochloride using winged needles. Plasma (60 μL) obtained from the blood sample was mixed with MeOH (200 μL) to remove plasma proteins and then centrifuged at 2000*g* for 3 min at room temperature in a microcentrifuge (MCF-2360, LMS Co., Ltd., Tokyo, Japan). A 228 μL aliquot of each supernatant was mixed with 12 μL of phenol in saline (stock solution: 0.3 mg/mL) to give a final concentration of phenol of 150 μg/mL, then filtered. A 200 μL aliquot of each filtrate was analyzed by HPLC using phenol as an internal standard. Compound **2** was detected in the HPLC analysis of each filtrate and its peak was characterized by ESI-TOF-MS. The HPLC of the filtrate prepared 30 min after administration of **2·HCl** is shown in Figure 5. Blood concentrations of compound **2** after 0.5, 1, 2, 4 or 24 h administration were calculated using the calibration curve (SD Fig. S6) and plotted as shown in Figure 6.

Using the time-course data, the half-life was calculated as 98.4 min by curve fitting based on GraphPad Prism Version 5.04 (GraphPad Software, CA, U.S.A.). The initial concentration in blood was also calculated as 1.50 μg/mL. In a macaque, this suggests that the renal excretion is not possible and this was by the absence of compound **2** in the HPLC analysis of the urine (SD). The distribution volume was calculated as 47.1 L; the dose 70.6 (mg)/initial concentration 1.50 (μg/mL) ratio suggests tissue distribution.

2.4. Adsorption of compound 2 to blood cells of a rhesus macaque

The question of whether compound **2** can be attached to and adsorbed into blood cells was investigated. Initially, **2·HCl** was added to blood (1 mL) of a rhesus macaque reaching a final concentration of 1 mg/mL. This mixture was incubated at 37 °C for 0, 1 and 2 h, and then centrifuged at 3600 rpm for 5 min at room temperature in a microcentrifuge to separate plasma (730 μL) from

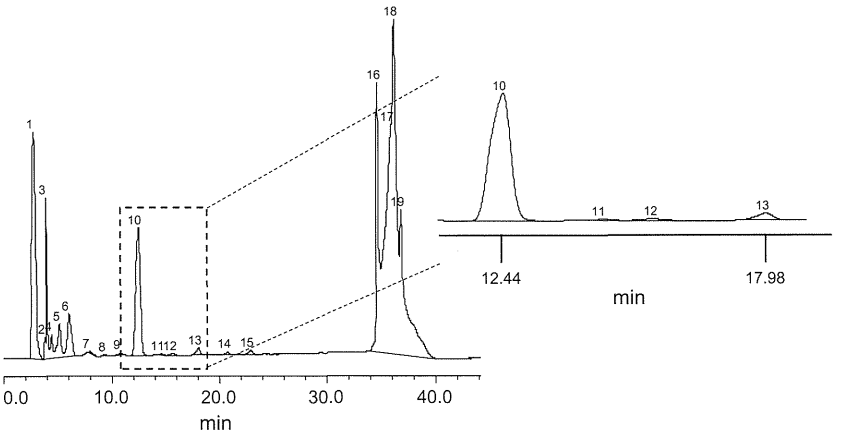

Figure 5. HPLC chart of macaque plasma 30 min after intravenous administration of **2·HCl**. The plasma sample was eluted with a linear gradient of 20–35% CH_3CN (0.1% TFA, in 30 min). Peak 10 (retention time: 12.44 min) corresponds to the internal standard (phenol) and peak 13 (retention time: 17.98 min) corresponds to compound **2**.

blood cells. In addition, plasma (0.5 mL) was added to the blood cells incubated for 1 h, then the mixture was incubated again for 1 h to separate plasma (730 μL) from the blood cells. Blood cell samples were prepared by mixing the blood cells with 480 μL of PBS and diluting the mixture to 1 mL with PBS. Blood cell samples were sonicated to disrupt cell membranes then both plasma and blood cell samples (60 μL each) were vortex-mixed with 200 μL of MeOH, then centrifuged at 2000*g* for 3 min at room temperature. A 228 μL aliquot of each supernatant was mixed with 12 μL of phenol in saline (final concentration: 600 μg/mL) and filtered. A 200 μL aliquot of each filtrate was injected to HPLC by an autosampler (SD Fig. S8).

The fractions of plasma and blood cells were analyzed by HPLC to quantify compound **2** (Fig. 7). The results showed that incubation enhanced the attachment or adsorption of compound **2** to blood cells; incubation for 1 or 2 h led to percentages of 39.7% and 39.3%, respectively, in distribution in cells, prior to incubation there was a distribution percentage of 34.8% in cells. Furthermore, compound **2**, which was adsorbed into blood cells, was significantly redistributed in plasma when fresh plasma was added; the addition of plasma to blood cells incubated for 1 h and a further incubation for 1 h caused redistribution of compound **2** to plasma and a reduction of distribution percentages to cells from 39.7% to 11.5%. This suggests that compound **2**, which was attached to blood cells, might be transferred from the cells to plasma and subsequently distributed to tissues.

These results indicate that the concentration in blood of compound **2** might be reduced, ultimately to ~1 mg/mL (3 μM) with 2–4 h treatments in rats (14 mg/kg) and rhesus macaques (13.4 mg/kg). The EC_{50} value of compound **2** has been determined as 10–50 μM in laboratory and primary HIV-1 strains.[11] Thus, in several hours after intravenous administration of compound **2** the efficacy might be diminished because the concentration in blood of compound **2** is being maintained below EC_{50} levels. However, the amount administered cannot be increased because of the acute toxicity which is described in the previous section, although the concentration in blood of compound **2** does not reach its CC_{50} level of 210 μM.[11] Recently, we reported that CD4 mimics such as compound **1** enhance the binding potency of anti-gp120 monoclonal antibodies such as KD-247[16] toward an envelope protein gp120, showing synergistic neutralization.[13] Compound **2** also enhances the neutralizing activity of KD-247 against simian–human immunodeficiency virus (SHIV)-KS661 strain via highly synergistic interactions. When compound **2** is used in combination with anti-gp120 monoclonal antibodies such as KD-247, the level of compound **2** of 3 μM might be sufficient for neutralization in vivo and thus it might be possible to reduce the dose of compound **2**. In addition, we also found that compound **1** and CXCR4 antagonists such as T140[2] showed synergistic anti-HIV-1 activity,[11] Thus, a combinatorial use with co-receptor antagonists would be also effective for reduction of the dose of compound **2**.

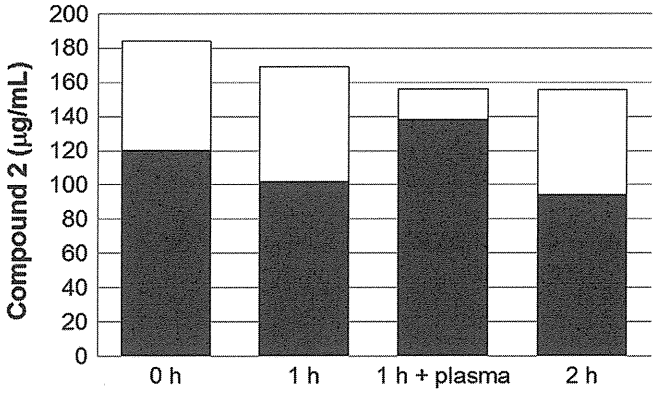

Figure 7. Quantitative analysis of compound **2** contained in macaque blood cells and plasma after incubation for 0, 1, or 2 h. 1 h + plasma means the addition of plasma (0.5 mL) to 1 h incubated blood cells followed by further incubation for 1 h. Concentrations of compound **2** in plasma are shown in black bars, and those in blood cells are shown in white bars.

3. Conclusion

CD4 mimics are attractive not only as HIV entry inhibitors but also possibly as cooperating agents for neutralizing antibodies. Binding of CD4 mimicking compounds to gp120 causes a conformational change in gp120. In this way, CD4 mimics function as 'envelope openers' and enhance the binding ability of anti-gp120 neutralizing antibodies. We discovered lead compound **2** with relatively high potency and low cytotoxicity in our previous study. In the current study, the pharmacokinetics of compound **2** in rats and rhesus macaques in the intravenous administration were investigated. Plots of plasma concentrations of compound **2** fitted with a one-compartment model provided calculation of half-lives of compound **2** in blood in rats and rhesus macaques: 8.4 and 98.4 min, respectively, suggesting that compound **2** is broadly distributed in tissues. A few hours post-injection, plasma concentrations of compound **2** in both species stabilized at micromolar levels. Consequently, compound **2** might have promise as a lead compound for the intravenous administration in a cocktail therapy with anti-gp120 monoclonal antibodies such as KD-247 and with co-receptor antagonists such as T140.[2]

4. Experimental

4.1. General information

A Cosmosil 5C18-ARII column (4.6 × 250 mm, Nacalai Tesque, Inc., Kyoto, Japan) was used for analytical HPLC, with a linear gradient of CH_3CN containing 0.1% (v/v) TFA at a flow rate of 1 cm^3 min^{-1} on a JASCO PU-2089 plus (JASCO Corporation, Ltd., Tokyo, Japan), and eluents were detected by UV at 220 nm on a JASCO UV-2075 plus (JASCO Corporation, Ltd, Tokyo, Japan). Samples were injected by an autosampler on a JASCO AS-2075 plus (JASCO Corporation, Ltd, Tokyo, Japan). ESI-TOF-MS were recorded on a micrOTOF-2focus (Bruker Daltonics) mass spectrometer.

4.2. Calibration curve

To compound **2** (1.0 g) in MeOH (5 mL) was added 4 M HCl/dioxane (10 mL) and the mixture was stirred for 30 min at room temperature. The mixture was concentrated under reduced pressure and the **2**·**HCl** was precipitated in cooled Et_2O (yield: 1.2 g, quantitative).

To construct a pharmacokinetics calibration curve in a rat, standard stock solutions in saline of **2**·**HCl**; 263, 131.5, 65.8, 32.9 and 16.4 μg/mL and an internal standard stock solution; 1.25 mg/mL phenol in saline were prepared. Each standard stock solution (22.8 μL) was mixed with 1.2 μL of the internal stock solution to give a total volume of 24 μL, then filtered. A 20 μL aliquot of each filtrate was injected to HPLC. The final concentration of **2**·**HCl** was 250, 125, 62.5, 31.3 or 15.6 μg/mL and each sample contains 62.5 μg/mL phenol. Elution was carried out with a linear gradient of 20–35% CH_3CN (0.1% TFA) over 30 min (SD Fig. S3). A calibration curve was constructed using the ratio of HPLC peak areas and concentrations of **2**·**HCl** to demonstrate the linearity as shown in Figure 2. The linear regression equation is $Y = 0.1345X$ ($R^2 = 0.9981$).

To construct a pharmacokinetics calibration curve in a rhesus macaque, standard stock solutions in saline of **2**·**HCl** (329, 164.5,

82.3, 41.1, 20.6 and 10.3 μg/mL) and an internal standard stock solution of phenol in saline (3 mg/mL) were prepared. Each standard stock solution (22.8 μL) was mixed with 1.2 μL of the internal stock solution and filtered. A 20 μL aliquot of each filtrate was injected to HPLC. The final concentration of **2·HCl** was 312.5, 156.3, 78.1, 39.1, 19.5 and 9.77 μg/mL, each contained 150 μg/mL phenol. Elution was carried out with a linear gradient of 20–35% CH_3CN (0.1% TFA) over 30 min. A calibration curve was constructed using the ratio of HPLC peak areas and concentrations of **2·HCl** to demonstrate the linearity as shown in SD Figure S5. The linear regression equation is $Y = 0.034X$ ($R^2 = 0.9927$).

To construct a calibration curve for the adsorption experiments, standard stock solutions in saline of **2·HCl**; 1000, 500, 250, 100, 50 μg/mL and an internal standard stock solution of 12 mg/mL phenol in saline were prepared. Each standard stock solution (228 μL) was mixed with 12 μL of the internal stock solution and filtered. A 200 μL aliquot of each filtrate was injected to HPLC by an autosampler. The final concentration of **2·HCl** was 950, 475, 238, 95.0 and 47.5 μg/mL and contained 600 μg/mL phenol. Elution was carried out with a linear gradient of 20–35% CH_3CN (0.1% TFA) over 30 min. A calibration curve was constructed using the ratio of HPLC peak areas and concentrations of **2·HCl** to demonstrate the linearity shown in SD Figure S7. The linear regression equation is $Y = 0.0553X$ ($R^2 = 0.9263$).

4.3. Pharmacokinetics in rats

Experiments using rats were conducted in an animal facility under specific pathogen-free conditions, in compliance with institutional regulations approved by the Committee of Tokyo Medical and Dental University (Tokyo, Japan). Five-week-old Jcl:SD rats purchased from CLEA Japan, Inc. (Tokyo, Japan) were maintained for one week before experiments. Compound **2·HCl** (2.5 mg) in 1.0 mL of saline was administered by tail vein injection into 6 week-old Jcl:SD rats. Blood was collected from the tail vein into centrifugal blood collection tubes (E·DS11, Eiken Chemical Co., Ltd., Tokyo, Japan) 15, 30, 45, 60, 120 and 240 min after administration. Blood was centrifuged at 2000*g* for 3 min at room temperature to separate plasma and stored at −80 °C before use. A freeze-thawed plasma sample (50 μL) was mixed with 10 μL of phenol in saline (stock solution: 0.375 mg/mL, giving a final concentration of 62.5 μg/mL) and filtered at 2000*g* for 3 min in a microcentrifuge (MCF-2360, LMS Co., Ltd., Tokyo, Japan). A 50 μL aliquot of each filtrate was injected into an HPLC. Elution was carried out with a linear gradient of 20–35% CH_3CN (0.1% TFA) over 30 min shown in SD Figure S4. Compound **2** was detected in the HPLC analysis and its peak was characterized by ESI-TOF-MS (*m/z* calcd for $C_{18}H_{28}N_3O_2$ $[M+H]^+$ 318.22, found 318.19).

4.4. Pharmacokinetics in a rhesus macaque

Experiments using an adult female rhesus macaque, seven years old, were conducted in a biosafety level 3 animal facility, in compliance with institutional regulations approved by the Committee for Experimental Use of Nonhuman Primates of the Institute for Virus Research, Kyoto University (Kyoto, Japan). Compound **2·HCl** (70.6 mg) in 30 mL of 0.1 M sodium phosphate buffer containing NaCl (pH 7.4) was administered by cephalic vein injection. Blood (3.0 mL) was collected from the cephalic vein 0, 0.5, 1, 2, 4 and 24 h after administration using winged needles. Blood was centrifuged at 3600 rpm for 5 min at room temperature to separate plasma then stored at −80 °C before use. A freeze-thawed plasma sample (60 μL) was vortex-mixed with MeOH (200 μL) and centrifuged at 2000*g* for 3 min at room temperature. A 228 μL aliquot of each supernatant was mixed with 12 μL of phenol in saline (stock solution: 0.3 mg/mL, final concentration: 150 μg/mL) and filtered. A 200 μL aliquot of each filtrate was injected into HPLC by an autosampler. Elution was carried out with a linear gradient of 20–35% CH_3CN (0.1% TFA) over 30 min shown in SD Figure S6. Compound **2** was detected in the HPLC analysis of each filtrate and its peak was characterized by ESI-TOF-MS (*m/z* calcd for $C_{18}H_{28}N_3O_2$ $[M+H]^+$ 318.22, found 318.19).

4.5. Adsorption experiments of compound 2 to blood cells of a rhesus macaque

Compound **2·HCl** in saline (5 mg/mL, 0.25 mL) was added to blood (1.0 mL) collected from a macaque, and incubated at 37 °C for 0, 1 and 2 h. After incubation, plasma samples (730 μL) were separated by centrifugation at 3600 rpm for 5 min at room temperature, and PBS (480 μL) was added to the resulting precipitates, increasing their total volume to 1.0 mL, and producing blood cell samples. In addition, plasma (0.5 mL) was added to the blood cells after 1 h incubation and the mixture was incubated again for 1 h to separate plasma (730 μL) and blood cells. The separated plasma and blood cell samples were stored at −80 °C before use. Freeze-thawed plasma samples (60 μL) were vortex-mixed with MeOH (200 μL) and centrifuged at 2000*g* for 3 min at room temperature. Freeze-thawed blood cell samples (200 μL) were sonicated to disrupt cell membranes (Sonifier 250, Branson Ultrasonics, Emerson Japan Ltd., Kanagawa, Japan), and 60 μL of the sonicated products was vortex-mixed with MeOH (200 μL) and centrifuged at 2000*g* for 3 min at room temperature. A 228 μL aliquot of each supernatant obtained from both plasma and blood cell samples was mixed with 12 μL of phenol in saline (stock solution: 12 mg/mL, final concentration: 600 μg/mL) and filtered. After filtration, a 200 μL aliquot of each filtrate was injected into HPLC by an autosampler. Elution was carried out with a linear gradient of 20–35% CH_3CN (0.1% TFA) over 30 min and is shown in SD Figure S8.

Acknowledgments

This work was supported in part by Grant-in-Aid for Scientific Research from the Ministry of Education, Culture, Sports, Science, and Technology of Japan, and Health and Labour Sciences Research Grants from Japanese Ministry of Health, Labor, and Welfare. The authors thank Ms. Misako Namae and Professor Hiroshi Nishina, Medical Research Institute, Tokyo Medical and Dental University, for providing us with methods for the collection of blood from rats. The authors also thank Dr. Fumiyoshi Yamashita, Graduate School of Pharmaceutical Sciences, Kyoto University, for assistance with the calculation of the pharmacokinetics. Our thanks are also extended to Ms. Yuko Yamada and Ms. Aki Ohya, from our laboratory, for teaching us techniques for analysis of plasma samples.

Supplementary data

Supplementary data (figures of changes on body weight and on intake amounts of bait and water in rats, tables of HPLC peak areas and HPLC charts) associated with this article can be found, in the online version, at http://dx.doi.org/10.1016/j.bmc.2013.10.005.

References and notes

1. Hashimoto, C.; Tanaka, T.; Narumi, T.; Nomura, W.; Tamamura, H. *Expert Opin. Drug Discovery* **2011**, *6*, 1067.
2. (a) Tamamura, H.; Xu, Y.; Hattori, T.; Zhang, X.; Arakaki, R.; Kanbara, K.; Omagari, A.; Otaka, A.; Ibuka, T.; Yamamoto, N.; Nakashima, H.; Fujii, N. *Biochem. Biophys. Res. Commun.* **1998**, *253*, 877; (b) Tamamura, H.; Omagari, A.; Oishi, S.; Kanamoto, T.; Yamamoto, N.; Peiper, S. C.; Nakashima, H.; Otaka, A.; Fujii, N. *Bioorg. Med. Chem. Lett.* **2000**, *10*, 2633; (c) Fujii, N.; Oishi, S.; Hiramatsu, K.; Araki, T.; Ueda, S.; Tamamura, H.; Otaka, A.; Kusano, S.; Terakubo, S.; Nakashima, H.; Broach, J. A.; Trent, J. O.; Wang, Z.; Peiper, S. C. *Angew. Chem., Int. Ed.* **2003**, *42*, 3251; (d) Tamamura, H.; Hiramatsu, K.; Ueda,

S.; Wang, Z.; Kusano, S.; Terakubo, S.; Trent, J. O.; Peiper, S. C.; Yamamoto, N.; Nakashima, H.; Otaka, A.; Fujii, N. *J. Med. Chem.* **2005**, *48*, 380; (e) Tamamura, H.; Araki, T.; Ueda, S.; Wang, Z.; Oishi, S.; Esaka, A.; Trent, J. O.; Nakashima, H.; Yamamoto, N.; Peiper, S. C.; Otaka, A.; Fujii, N. *J. Med. Chem.* **2005**, *48*, 3280.

3. Chan, D. C.; Kim, P. S. *Cell* **1998**, *93*, 681.
4. Eckert, D. M.; Kim, P. S. *Annu. Rev. Biochem.* **2001**, *70*, 777.
5. Wyatt, R.; Sodroski, J. *Science* **1884**, *1998*, 280.
6. Berger, E. A.; Murphy, P. M.; Farber, J. M. *Annu. Rev. Immunol.* **1999**, *17*, 657.
7. (a) Wild, C. T.; Shugars, D. C.; Greenwell, T. K.; McDanal, C. B.; Matthews, T. J.; Chan, D. C.; Fass, D. *Proc. Natl. Acad. Sci. U.S.A.* **1994**, *91*, 9770; (b) Berger, J. M.; Kim, P. S. *Cell* **1997**, *89*, 263; (c) Otaka, A.; Nakamura, M.; Nameki, D.; Kodama, E.; Uchiyama, S.; Nakamura, S.; Nakano, H.; Tamamura, H.; Kobayashi, Y.; Matsuoka, M.; Fujii, N. *Angew. Chem., Int. Ed.* **2002**, *41*, 2937; (d) Nomura, W.; Hashimoto, C.; Ohya, A.; Miyauchi, K.; Urano, E.; Tanaka, T.; Narumi, T.; Nakahara, T.; Komano, J. A.; Yamamoto, N.; Tamamura, H. *ChemMedChem* **2012**, *7*, 205; (e) Hashimoto, C.; Nomura, W.; Ohya, A.; Urano, E.; Miyauchi, K.; Narumi, T.; Aikawa, H.; Komano, J. A.; Yamamoto, N.; Tamamura, H. *Bioorg. Med. Chem.* **2012**, *20*, 3287; (f) Nomura, W.; Hashimoto, C.; Suzuki, T.; Ohashi, N.; Fujino, M.; Murakami, T.; Yamamoto, N.; Tamamura, H. *Bioorg. Med. Chem.* **2013**, *21*, 4452.
8. Zhao, Q.; Ma, L.; Jiang, S.; Lu, H.; Liu, S.; He, Y.; Strick, N.; Neamati, N.; Debnath, A. K. *Virology* **2005**, *339*, 213.
9. (a) Madani, N.; Schön, A.; Princiotto, A. M.; LaLonde, J. M.; Courter, J. R.; Soeta, T.; Ng, D.; Wang, L.; Brower, E. T.; Xiang, S.-H.; Do Kwon, Y.; Huang, C.-C.; Wyatt, R.; Kwong, P. D.; Freire, E.; Smith, A. B., 3rd; Sodroski, J. *Structure* **2008**, *16*, 1689; (b) LaLonde, J. M.; Elban, M. A.; Courter, J. R.; Sugawara, A.; Soeta, T.; Madani, N.; Princiotto, A. M.; Kwon, Y. D.; Kwong, P. D.; Schön, A.; Freire, E.; Sodroski, J.; Smith, A. B., 3rd *Bioorg. Med. Chem. Lett.* **2011**, *20*, 354; (c) LaLonde, J. M.; Kwon, Y. D.; Jones, D. M.; Sun, A. W.; Courter, J. R.; Soeta, T.; Kobayashi, T.; Princiotto, A. M.; Wu, X.; Schön, A.; Freire, E.; Kwong, P. D.; Mascola, J. R.; Sodroski, J.; Madani, N.; Smith, A. B., 3rd *J. Med. Chem.* **2012**, *55*, 4382.
10. Curreli, F.; Choudhury, S.; Pyatkin, I.; Zagorodnikov, V. P.; Bulay, A. K.; Altieri, A.; Kwon, Y. D.; Kwon, P. D.; Debnath, A. K. *J. Med. Chem.* **2012**, *55*, 4764.
11. (a) Yamada, Y.; Ochiai, C.; Yoshimura, K.; Tanaka, T.; Ohashi, N.; Narumi, T.; Nomura, W.; Harada, S.; Matsushita, S.; Tamamura, H. *Bioorg. Med. Chem. Lett.* **2010**, *20*, 354; (b) Narumi, T.; Ochiai, C.; Yoshimura, K.; Harada, S.; Tanaka, T.; Nomura, W.; Arai, H.; Ozaki, T.; Ohashi, N.; Matsushita, S.; Tamamura, H. *Bioorg. Med. Chem. Lett.* **2010**, *20*, 5853; (c) Narumi, T.; Arai, H.; Yoshimura, K.; Harada, S.; Nomura, W.; Matsushita, S.; Tamamura, H. *Bioorg. Med. Chem.* **2011**, *19*, 6735; (d) Narumi, T.; Arai, H.; Yoshimura, K.; Harada, S.; Hirota, Y.; Ohashi, N.; Hashimoto, C.; Nomura, W.; Matsushita, S.; Tamamura, H. *Bioorg. Med. Chem.* **2013**, *21*, 2518.
12. Schön, A.; Madani, N.; Klein, J. C.; Hubicki, A.; Ng, D.; Yang, X.; Smith, A. B., 3rd; Sodroski, J.; Freire, E. *Biochemistry* **2006**, *45*, 10973; (b) Schön, A.; Lam, S. Y.; Freire, E. *Future Med. Chem.* **2011**, *3*, 1129.
13. Yoshimura, K.; Harada, S.; Shibata, J.; Hatada, M.; Yamada, Y.; Ochiai, C.; Tamamura, H.; Matsushita, S. *J. Virol.* **2010**, *84*, 7558.
14. Mao, S.; Jin, H.; Bi, Y.-Q.; Liang, Z.; Li, H.; Hou, S.-X. *Chem. Pharm. Bull.* **2007**, *55*, 753.
15. Sakai-Kato, K.; Nanjo, K.; Kawanishi, T.; Okuda, H. *Chem. Pharm. Bull.* **2012**, *60*, 391.
16. Eda, Y.; Takizawa, M.; Murakami, T.; Maeda, H.; Kimachi, K.; Yonemura, H.; Koyanagi, S.; Shiosaki, K.; Higuchi, H.; Makizumi, K.; Nakashima, T.; Osatomi, K.; Tokiyoshi, S.; Matsushita, S.; Yamamoto, N.; Honda, M. *J. Virol.* **2006**, *80*, 5552.

Journal of General Virology (2013), **94**, 2710–2716 DOI 10.1099/vir.0.055590-0

Short Communication

Generation of a replication-competent simian–human immunodeficiency virus, the neutralization sensitivity of which can be enhanced in the presence of a small-molecule CD4 mimic

Hiroyuki Otsuki,[1] Takayuki Hishiki,[1] Tomoyuki Miura,[1] Chie Hashimoto,[2] Tetsuo Narumi,[2] Hirokazu Tamamura,[2] Kazuhisa Yoshimura,[3] Shuzo Matsushita[4] and Tatsuhiko Igarashi[1]

Correspondence
Tatsuhiko Igarashi
tigarash@virus.kyoto-u.ac.jp

[1]Laboratory of Primate Model, Experimental Research Center for Infectious Diseases, Institute for Virus Research, Kyoto University, Kyoto 606-8507, Japan

[2]Department of Medicinal Chemistry, Institute of Biomaterials and Bioengineering, Tokyo Medical and Dental University, Tokyo 101-0062, Japan

[3]AIDS Research Center, National Institute of Infectious Diseases, Tokyo 162-8640, Japan

[4]Division of Clinical Retrovirology and Infectious Diseases, Center for AIDS Research, Kumamoto University, Kumamoto 860-0811, Japan

Received 29 May 2013
Accepted 10 September 2013

Simian–human immunodeficiency virus (SHIV) carrying the envelope from the clade B clinical human immunodeficiency virus type 1 (HIV-1) isolate MNA, designated SHIV MNA, was generated through intracellular homologous recombination. SHIV MNA inherited biological properties from the parental HIV-1, including CCR5 co-receptor preference, resistance to neutralization by the anti-V3 loop mAb KD-247 and loss of resistance in the presence of the CD4-mimic small-molecule YYA-021. SHIV MNA showed productive replication in rhesus macaque PBMCs. Experimental infection of a rhesus macaque with SHIV MNA caused a transient but high titre of plasma viral RNA and a moderate antibody response. Immunoglobulin in the plasma at 24 weeks post-infection was capable of neutralizing SHIV MNA in the presence but not in the absence of YYA-021. SHIV MNA could serve a model for development of novel therapeutic interventions based on CD4-mimic-mediated conversion of envelope protein susceptible to antibody neutralization.

Control of primate lentiviral infection by antibodies directed against viral envelope protein is theoretically feasible. This was confirmed by the successful protection of macaque monkeys from challenge inoculation with simian–human immunodeficiency virus (SHIV) carrying an envelope protein (Env). Env was derived from a laboratory strain of human immunodeficiency virus type 1 (HIV-1) through the passive immunization of neutralizing mAbs directed against HIV-1 (Mascola *et al.*, 2000; Nishimura *et al.*, 2003). This neutralization is consistent with the results normally seen in cell culture systems.

In contrast, clinical isolates of HIV-1 that have not been subjected to extensive passage in T-cell lines are generally resistant to antibody-mediated neutralization (Moore *et al.*, 1995). It has been shown that virus in infected individuals is under selective pressure to develop a variety of means to evade attack by neutralizing antibodies, including sequence variation, glycosylation, tertiary structural shielding formed by the Env trimer and the rapid kinetics of conformational changes of Env, which affect fusion between the viral envelope and the plasma membrane of target cells (Kong & Sattentau, 2012). Although four major neutralizing epitopes have been identified in HIV-1 Env (i.e. the V1/V2 loop, the glycan-V3 site and CD4-binding site of gp120, and the membrane-proximal external region of gp41), for reasons that are as yet unclear few reports of antibodies directed against these epitopes capable of neutralizing a broad range of isolates have been published (Kwong & Mascola, 2012). High titres of antibodies directed against the V3 loop are elicited in individuals during the early phase of HIV-1 infection, but these are incapable of neutralizing the virus because the epitope in functional Env trimer is probably shielded from the antibody (Davis *et al.*, 2009b). Therefore, it is necessary to develop a means of rendering these epitopes accessible to

One supplementary table and five supplementary figures are available with the online version of this paper.

the antibodies, to make antibody-mediated suppression of HIV-1 a valid therapeutic option.

It has been reported that neutralization mediated by antibodies directed against the V3 loop (Lusso *et al.*, 2005) or CD4-induced epitope (CD4i) (Thali *et al.*, 1993) can be enhanced in the presence of soluble CD4 (sCD4). It is known that the interaction of Env with sCD4 drives a conformational change of the viral protein and makes the cryptic/occult epitopes accessible to these antibodies (Wyatt *et al.*, 1998). Small molecules that emulate sCD4 for its interaction and subsequent induction of conformational change of Env may be employed to intensify antibody-mediated interventions against HIV-1 infection. Compounds with the above-mentioned properties (i.e. NBD-556 and NBD-557) have been reported previously (Zhao *et al.*, 2005). NBD-556 has been shown in cell culture to interact with the CD4-binding pocket to induce a conformational change in gp120 (Madani *et al.*, 2008) and enhance exposure of the Env of primary HIV-1 isolates to neutralizing epitopes (Yoshimura *et al.*, 2010).

The present study was performed to evaluate small-molecule CD4-mimic-based enhancement of antibody-mediated virus neutralization, in the context of virus infection *in vivo*. The SHIV/macaque monkey model of AIDS is particularly suitable for such studies, as SHIV carries the HIV-1 Env and the neutralization sensitivity of SHIV is comparable to that of the parental HIV-1 (Shibata & Adachi, 1992).

As NBD-556, unlike sCD4, inhibits infection with select HIV-1 isolates (Yoshimura *et al.*, 2010), we generated a new SHIV strain carrying Env, the sensitivity of which to antibody-mediated neutralization is enhanced in the presence of a CD4 mimic. An HIV-1 isolate (MNA), previously designated primary isolate HIV-1 Pt.3, was used as the source of Env, as the viral protein has been reported to interact with NBD-556 (Yoshimura *et al.*, 2010). While the virus belongs to a distinct subset of HIV-1 isolates, as mentioned above, it has also been reported to utilize the CCR5 molecule to gain entry into target cells, a property that is shared by the majority of HIV-1 strains (Yoshimura *et al.*, 2010). A mAb directed against the tip of the V3 loop (GPGR motif), KD-247 (Eda *et al.*, 2006), was employed to assess this concept, as HIV-1 MNA is resistant to KD-247-mediated neutralization, despite carrying the exact epitope sequence in the tip of the V3 loop, and is converted to being sensitive to the antibody by NBD-556 in a dose-dependent manner (Yoshimura *et al.*, 2010).

First, we reproduced the results of Yoshimura *et al.* (2010) using a neutralization assay employing TZM-bl cells (Platt *et al.*, 1998), obtained from the National Institutes of Health (NIH) AIDS Reagent Program (Fig. S1, available in JGV Online). The virus was resistant to KD-247, as described previously, and required almost 50 μg ml^{-1} of the antibody to achieve 50 % neutralization in our assay. However, the observed resistance was eliminated in the presence of 2 μM NBD-556; 50 % neutralization was achieved in the presence of ~0.1 μg KD-247 ml^{-1}, corresponding to 1/500 of the amount of the antibody to achieve the same degree of neutralization in the absence of the CD4 mimic.

With reproduction of the properties of HIV-1 MNA Env, we generated an SHIV strain carrying Env through intracellular homologous recombination, as described previously (Fujita *et al.*, 2013) with minor modifications (Fig. S2). DNA fragments representing the 5′ and 3′ ends of the SHIV genome (fragments I and II, respectively) were amplified by PCR from the proviral DNA plasmid SHIV KS661. A DNA fragment containing *env* (fragment III) was amplified from cDNA of the HIV-1 MNA genome, which was prepared from virus particles (virion-associated RNA) in the culture supernatant of PM1/CCR5 cells (Yusa *et al.*, 2005) infected with the virus. The PCR primers used are listed in Table S1. Using a FuGENE HD transfection reagent, lipofection was performed on the C8166-CCR5 cells (Shimizu *et al.*, 2006) to co-transfect them with 0.2 μg DNA. A cytopathic effect, presumably caused by the emerged recombinant virus, was observed on day 13 post-transfection. The emerged virus, designated SHIV MNA, carried the entire gp120 and three-quarters of gp41 from HIV-1 MNA Env (Fig. 1a). The rest of Env was from SHIV KS661, the Env of which was derived from HIV-1 89.6 (Shinohara *et al.*, 1999). The CD4 binding site, and the regions and elements that reportedly interact with NBD-556 (Madani *et al.*, 2008; Yoshimura *et al.*, 2010), are preserved in SHIV MNA Env (Fig. S3). The virus was replication competent in PM1/CCR5 cells (data not shown).

As HIV-1 MNA has been suggested to be a CCR5-utilizing virus, we were intrigued as to whether SHIV MNA inherited the trait from the parental virus. We subjected SHIV MNA and the parental HIV-1 MNA to a co-receptor usage assay as described previously (Nishimura *et al.*, 2010), with minor modifications (Fig. S4). As expected, SHIV MNA was shown to utilize CCR5 as an entry co-receptor.

We next assessed the neutralization profiles of SHIV MNA in comparison with the parental HIV-1 MNA, as described previously (Li *et al.*, 2005; Wei *et al.*, 2002). Both SHIV MNA and HIV-1 MNA showed essentially no neutralization by KD-247 up to 25 μg ml^{-1}, and 50 % neutralization was achieved at 50 μg ml^{-1} (Fig. 1b). As the CD4 mimic, we employed YYA-021, a compound generated and characterized through studies concerning the structure–activity relationships of small molecules (Narumi *et al.*, 2010, 2011, 2013; Yamada *et al.*, 2010). The compound was shown to be slightly less potent but to exhibit substantially lower toxicity than NBD-556, and was therefore a suitable choice for our purposes in future studies in animal models. SHIV MNA was resistant to neutralization by YYA-021 at all concentrations examined, except 25 and 50 μM, and showed a neutralization profile almost identical to that of HIV-1 MNA (Fig. 1c). To further characterize the

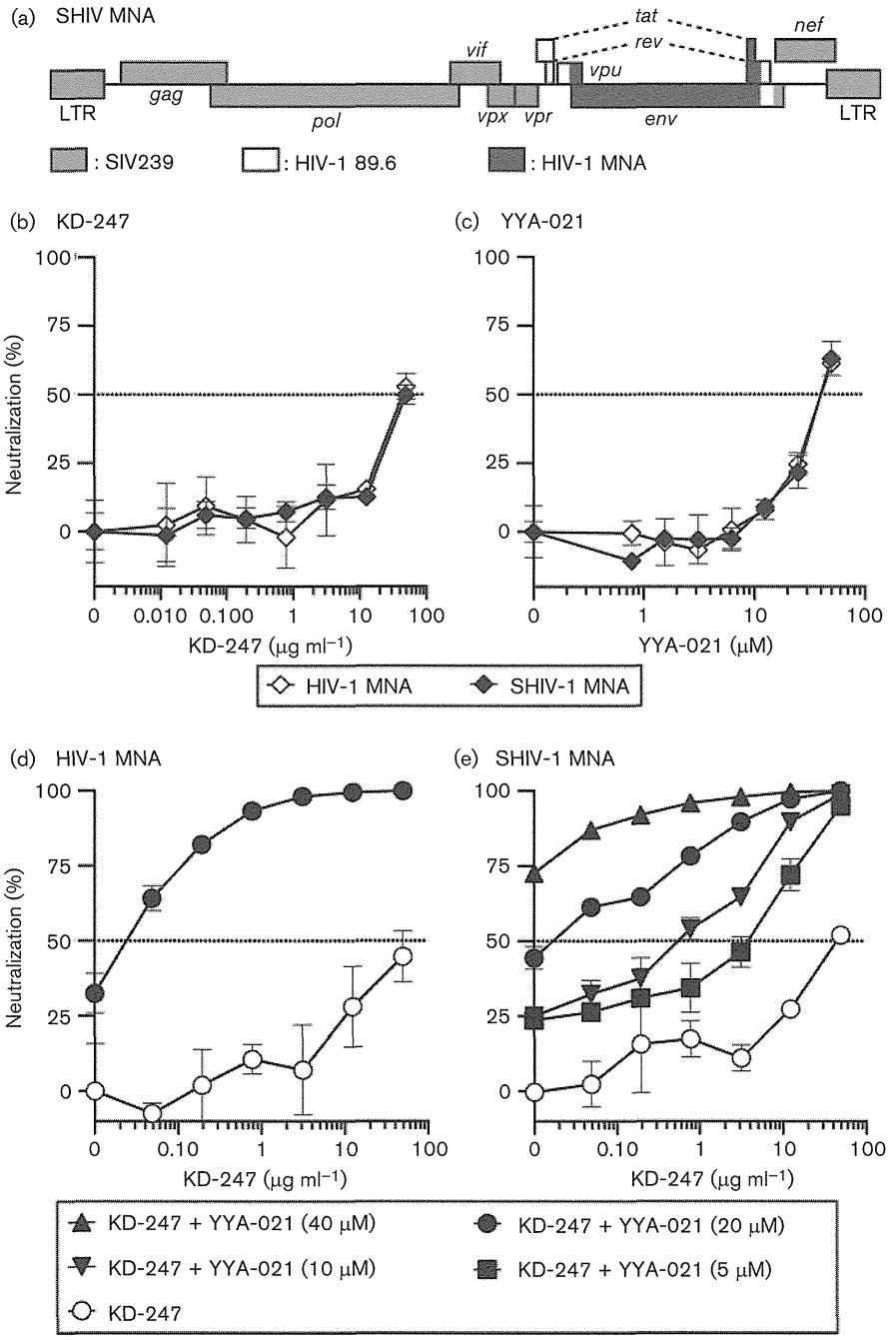

Fig. 1. Genomic organization (a) and neutralization sensitivity (b–e) of SHIV MNA. (a) Grey shaded boxes represent genes derived from SIV239, open boxes those from HIV-1 89.6 and dark grey shaded boxes those from HIV-1 MNA. LTR, long terminal repeat. (b–e) Percentage neutralization was calculated as 100×[1−(RLU.N−RLU.B)/(RLU.V−RLU.B)], where RLU is relative luciferase units; RLU.N is RLU in wells with cells, virus and KD-247 and/or YYA-021; RLU.V is RLU in wells with cells and virus; and RLU.B is RLU in wells with cells.

biological properties of SHIV MNA Env, a set of entry assays was conducted (Fig. S5). The *env* genes cloned from SHIV MNA and HIV-1 MNA were utilized to generate pseudotyped viruses. These pseudotypes were inoculated into TZM-bl cells in the presence of increasing amounts of NBD-556, YYA-021 or sCD4. A control group was derived from another virus preparation pseudotyped with amphotropic murine leukemia virus (A-MLV) Env (Landau *et al.*, 1991). When the efficiency of entry was defined by intracellular luciferase activities, virtually no difference was observed between Envs of SHIV MNA and the parental HIV-1. Thus, SHIV MNA Env replicated in

C8166-CCR5 cells retained sensitivity to small-molecule CD4 mimics and sCD4 comparable to that of HIV-1 MNA.

We then examined whether the synergistic neutralization of HIV-1 MNA by KD-247 antibody in the presence of NBD-556 (Yoshimura *et al.*, 2010) would be reproduced when CD4 mimic was substituted by YYA-021. The synergistic neutralization effect of KD-247 and YYA-021 was reproduced in our experiments (Fig. 1d). At 50 μg ml^{-1}, KD-247 barely achieved 50 % neutralization of HIV-1 MNA but resulted in 50 % neutralization at <0.05 μg ml^{-1} in the presence of 20 μM of YYA-021.

Finally, to examine whether these two agents neutralized SHIV MNA in the same manner as the parental HIV-1, we conducted a neutralization assay with KD-247 in the presence of increasing amounts of YYA-021 (0, 5, 10, 20 and 40 μM) (Fig. 1e). The neutralization curve of KD-247 against SHIV MNA showed an upward shift as the concentration of YYA-021 increased (Fig. 1e), similar to the observations with HIV-1 (Fig. 1d), indicating augmentation of neutralization, and complete neutralization of both viruses was achieved at 20 μM YYA-021 (Fig. 1d, e). Based on these results, we concluded that the neutralization profile of SHIV MNA was comparable to that of HIV-1 MNA.

Reproduction of the neutralization characteristics of HIV-1 MNA in the newly generated SHIV prompted us to assess the ability of SHIV MNA to replicate in monkey cells. SHIV MNA, along with SIV239 and SHIV KS661, were normalized with infectious titres and inoculated into rhesus macaque PBMC preparations from four animals,

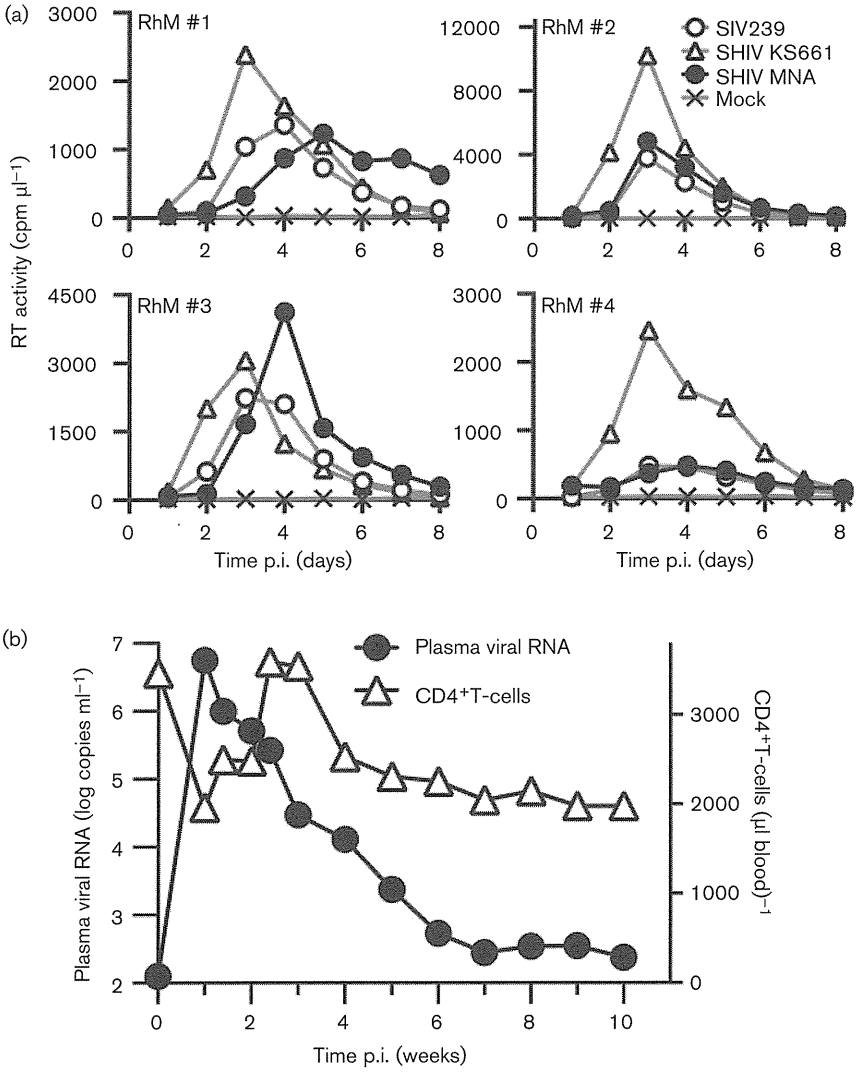

Fig. 2. Replication of SHIV MNA in rhesus macaque PBMCs (a) and *in vivo* (b). (a) M.o.i. was adjusted to 0.01 ($TCID_{50}$ per cell). (b) Experimental infection of a rhesus macaque with SHIV MNA. SHIV MNA (1.75×10^5 $TCID_{50}$) was intravenously inoculated into a rhesus macaque, and the plasma viral RNA burden and circulating $CD4^+$ T-lymphocytes were monitored.

as described previously (Fujita *et al.*, 2013) (Fig. 2a). SHIV KS661, a CXCR4-utilizing virus, replicated to the highest titres of all the viruses in all PBMC preparations. Compared with SHIV KS661, SIV239 replicated to lower titres. Under these experimental conditions, SHIV MNA showed productive replication in the cells with similar replication kinetics and peak titres to SIV239. Based on these results, we concluded that SHIV MNA was replication competent in primary monkey lymphocytes.

Productive replication of SHIV MNA in monkey PBMCs justified experimental infection of the virus *in vivo*. We inoculated 1.75×10^5 $TCID_{50}$ SHIV MNA intravenously into a rhesus macaque and monitored plasma viral RNA burden and circulating $CD4^+$ T-lymphocyte levels (Fig. 2b). Plasma viral RNA burden reached a peak of 5.6×10^6 copies ml^{-1} at 1 week post-infection (p.i.), and declined rapidly thereafter, reaching low levels of detection at 7 weeks p.i. (around 2.8×10^2 copies ml^{-1}). Circulating $CD4^+$ T-cell numbers showed a transient decrease around 1 week p.i., rebounded around 3 weeks p.i. and stabilized around 70 % of the pre-infection level from 4 weeks p.i. During the period of observation, the animal developed no obvious clinical manifestations related to lentivirus infection.

As SHIV MNA replicated *in vivo* without depleting helper T-cells, it was expected that the animal mounted an antiviral immune reaction. The production of antibody directed against Env was assessed by Western blotting, as described previously (Igarashi *et al.*, 1999). Purified Env protein (Advanced Biotechnologies) was used as the antigen (Fig. 3a). Anti-Env antibody was detected at 3 weeks p.i., and the level of antibody judged by the intensity of the band increased gradually with time.

We next examined whether the animal generated neutralizing antibodies against SHIV MNA. Because plasma samples from this specimen exhibited high background activity, IgG was purified from these samples collected on day 0 and in week 24 p.i. using protein G spin columns (GE Healthcare Japan). While the IgG from day 0 exhibited no neutralizing activity (Fig. 3b), as expected, the IgG collected at 24 weeks p.i. neutralized SHIV MNA, although a concentration >100 μg ml^{-1} was required to suppress replication of 100 $TCID_{50}$ of the input virus (Fig. 3c).

We examined whether the observed marginal neutralization by the antibody could be enhanced by the presence of YYA-021. Upon addition of YYA-021 in the assay system, SHIV MNA became sensitive to IgG obtained at 24 weeks p.i. (Fig. 3c), while no enhancement was identified from day 0 (Fig. 3b).

In this study, we generated a replication-competent SHIV MNA strain carrying an Env resistant to the neutralizing mAb KD-247 but conditionally sensitive in the presence of the CD4 mimic YYA-021. As the observed neutralization characteristics were identical to those of HIV-1 MNA, which contributed the majority of the Env sequence to the chimaera, the utility of the CD4 mimic as a means of enhancing antibody-mediated virus neutralization should be assessed in the context of infection *in vivo*. This concept could be tested during the acute phase of SHIV MNA infection, during which the virus undergoes substantial replication. To examine the feasibility of CD4-mimic-mediated enhancement of virus neutralization in the context of chronic infection, the conditions under which this type of intervention should be applied to HIV-1-infected patients in a clinical setting, the virus must be

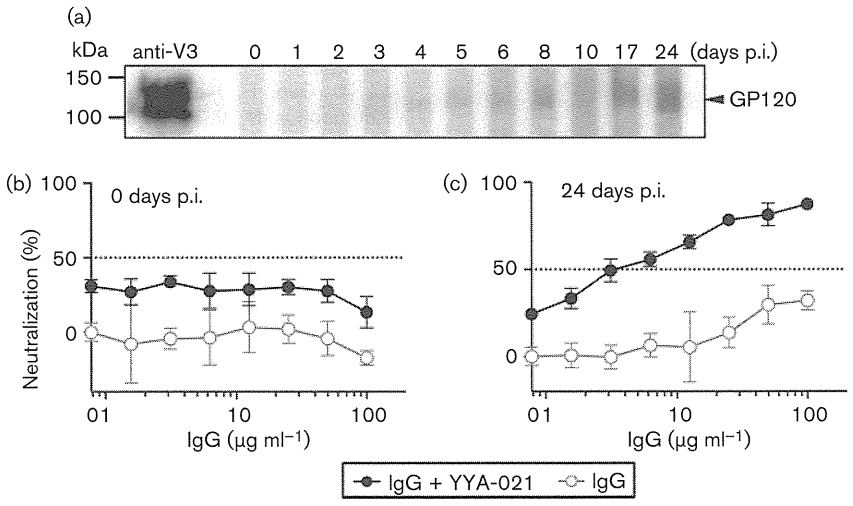

Fig. 3. Antibody induced against SHIV MNA. (a) The anti-HIV-1 gp120 antibody response was assessed by Western blotting with plasma samples collected at the indicated times. An anti-HIV-1 V3 mAb, 4G10 (ascites diluted 1 : 100) (von Brunn *et al.*, 1993), obtained from the NIH AIDS Reagent Program, was used as a positive control (lane anti-V3). (b, c) Neutralization of SHIV MNA with IgG purified from plasma of the infected rhesus macaque (day 0 and week 24 p.i.) with 20 μM YYA-021 or without YYA-021.